AD-A160 211 FRONTAL PASSAGE DATA FROM THE SOUSY-VHF-RADAR(U) 1/1
CORNELL UNIV ITHACA NY SCHOOL OF ELECTRICAL ENGINEERING
D T FARLEY AUG 85 AFOSR-TR-85-0852 AFOSR-83-0100

UNCLASSIFIED F/G 4/2 NL

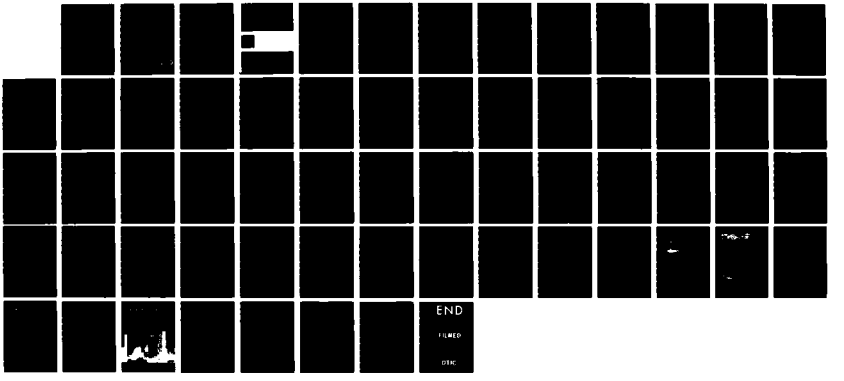

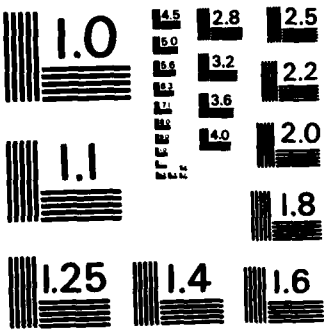

MICROCOPY RESOLUTION TEST CHART
NATIONAL BUREAU OF STANDARDS - 1963 - A

SECURITY

AD-A160 211

DOCUMENTATION PAGE

1a. REPORT SECURITY CLASSIFICATION: Unclassified	1b. RESTRICTIVE MARKINGS
2a. SECURITY CLASSIFICATION AUTHORITY	3. DISTRIBUTION/AVAILABILITY OF REPORT: Approved for public release; distribution unlimited
2b. DECLASSIFICATION/DOWNGRADING SCHEDULE	
4. PERFORMING ORGANIZATION REPORT NUMBER(S)	5. MONITORING ORGANIZATION REPORT NUMBER(S): AFOSR-TR- 85 0852
6a. NAME OF PERFORMING ORGANIZATION: Cornell University; 6b. OFFICE SYMBOL (If applicable)	7a. NAME OF MONITORING ORGANIZATION: AFOSR
6c. ADDRESS (City, State and ZIP Code): Phillips Hall, Ithaca, NY 14853	7b. ADDRESS (City, State and ZIP Code): Bldg 410, Bolling AFB DC 20332-6448
8a. NAME OF FUNDING/SPONSORING ORGANIZATION: AFOSR; 8b. OFFICE SYMBOL (If applicable): NC	9. PROCUREMENT INSTRUMENT IDENTIFICATION NUMBER: AFOSR 83-0100
8c. ADDRESS (City, State and ZIP Code): Bldg 410, Bolling AFB, DC 20332-6448	10. SOURCE OF FUNDING NOS.

PROGRAM ELEMENT NO.	PROJECT NO.	TASK NO.	WORK UNIT NO.
61102F	2310	A1	

11. TITLE (Include Security Classification): FRONTAL PASSAGE DATA FROM THE SOUSY-VHF-RADAR

12. PERSONAL AUTHOR(S): FARLEY D. T.

13a. TYPE OF REPORT	13b. TIME COVERED	14. DATE OF REPORT (Yr., Mo., Day)	15. PAGE COUNT
FINAL	FROM 1 Mar 83 TO 28 Feb 85	Aug 85	60

16. SUPPLEMENTARY NOTATION

17. COSATI CODES			18. SUBJECT TERMS (Continue on reverse if necessary and identify by block number)
FIELD	GROUP	SUB. GR.	

19. ABSTRACT (Continue on reverse if necessary and identify by block number)

Expirements have shown that there may be advantages in using a spaced antenna method instead of a Doppler mothod for measuring wind profiles, particularly for systems with small dimensions of the type likely to be used in operational wind profiling. The comparison between radar and radiosonde data have shown good agreement, indicating that the features seen in the radar reflectivity data are characteristic of frontal temperature structure and not associated with precipitation or local convection. Experiments show that a VHF radar operated continuously can provide synoptically meanigful meteorological data and is capable of high time resolution data required by future numerical methods.

20. DISTRIBUTION/AVAILABILITY OF ABSTRACT	21. ABSTRACT SECURITY CLASSIFICATION
UNCLASSIFIED/UNLIMITED [X] SAME AS RPT. [ ] DTIC USERS [ ]	Uncl.

22a. NAME OF RESPONSIBLE INDIVIDUAL	22b. TELEPHONE NUMBER (Include Area Code)	22c. OFFICE SYMBOL
Lt. Col. Ditteberner	(202) 767-4960	NC

DD FORM 1473, 83 APR EDITION OF 1 JAN 73 IS OBSOLETE.

Uncl.
SECURITY CLASSIFICATION OF THIS PAGE

SCHOOL OF ELECTRICAL ENGINEERING
Cornell University
PHILLIPS HALL
ITHACA, NEW YORK 14853

AFOSR-TR- 85-0852

August 13, 1985

To: Lt. Col. Gerald J. Dittberner
Program Manager
Directorate of Chemical and Atmospheric Sciences
AFOSR
Bolling Air Force Base, D.C. 20332-6448

From: D.T. Farley

Re: Final Technical Report, AFOSR 83-0100
Frontal Passage Data from the SOUSY-VHF-Radar

This grant, with a renewal, covered the period 1 March 1983 to 28 February 1985. The research supported by this grant was carried out by Dr. Miguel Larsen, who was a Research Associate at Cornell for most of the period of the grant until he left to become an Assistant Professor at Clemson University in the middle of August 1984. The research led to a number of publications, several of them in collaboration with Jurgen Rottger, a member of the German group that designed and built the SOUSY radar. The work covered both the science of meteorology and technical problems associated with radar probing of the atmosphere. The attached manuscripts and abstracts give a good idea of the results obtained.

The last experimental campaign carried out under this grant took place in April 1984. A number of interesting frontal passages were observed with the radar, in particular some unusual features somewhat arbitrarily called "mini-fronts", which are wavelike in character with downward sloping bands of enhanced reflectivity. Larsen is planning to continue the analysis of these results at Clemson.

D. T. Farley
Professor

Frank Feocco
Associate Director
Office of Sponsored Programs

Attachments

85 10 11 109

W O R L D M E T E O R O L O G I C A L O R G A N I Z A T I O N

PROGRAMME ON SHORT- AND MEDIUM-RANGE WEATHER PREDICTION RESEARCH (PSMP)

Potential Advantages of the Spaced Antenna Method for Operational Wind Profiling

J. Rottger[1] and M. F. Larsen[2]

1. Introduction

The problem of very short-range forecasting is twofold. It is necessary to understand the processes that are being forecasted, and data appropriate to the scale of interest has to be generated . Coherent VHF and UHF radars are being used for operational wind profiling and are providing part of the solution to the data acquisition problem (Larsen, 1983). The Profiler system operated by the Wave Propagation Laboratory at NOAA has already shown great promise (Strauch, 1981; Strauch et al., 1982). As a result, plans are being considered for expanding the network of radars to cover a larger area of the country.

The Profiler uses what is commonly referred to as the Doppler method for measuring winds. Two beams are pointed off-vertical, and the Doppler shift of the echo determines the line-of-sight velocity. The velocity components along the beams are then translated to horizontal wind components. While there is no doubt that the Doppler method is adequate for wind profiling, we want to discuss a number of possible advantages of the spaced antenna (SA) method for operational wind profiling. There is virtually no difference in cost between the two types of systems. However, there may be some significant advantages of the SA method, particularly when smaller radars are being considered. Since any Profiler network is still only in the planning stage, now is the time to consider the various alternatives.

2. Description of the two techniques

The Doppler method uses the same antenna array for transmitting and receiving. The array is phased in such a way that the beams point at some angle off vertical. The Doppler shift of the received signal is then proportional to the line-of-sight velocity, V' in the right-hand-side of Figure 1. Two beams pointing in different directions have to be used, together with the assumption that the vertical velocity is negligible, to determine the two horizontal wind components. The three-dimensional vector wind velocity can be determined uniquely only if three beam directions are used.

[1]EISCAT Scientific Association, P. O. Box 705, S-98127 Kiruna, Sweden, on leave from Max-Planck-Institut fur Aeronomie, D-3411 Katlenburg-Lindau, W. Germany
[2]School of Electrical Engineering, Cornell University, Ithaca, NY 14853

The spaced antenna method (see Röttger, 1981a for a detailed description), shown in the left-hand-side of Figure 1, uses one transmitter array and three closely spaced receiving arrays with all beams pointing vertically. The three receiving antennas may be separated from the transmitting antenna, but more efficient is a configuration in which each third of the transmitting array is used as a separate receiving array. The horizontal velocities are calculated using the time lags at which the cross-correlations of the signals received in the various antennas maximize. The spaced antenna method essentially tracks the propagation of a perturbation in the refractive index across the distance separating the receiving antennas. The vertical velocity is calculated from the Doppler shift.

An objection to the spaced antenna method that is often heard is that the technique gives incorrect wind measurements when the medium is strongly affected by wave activity. In that case the scattering is primarily from the refractive index structure associated with the wave fronts, and the measured velocity is the phase velocity of the waves rather than the true wind velocity. However, Briggs (1980) has shown rigorously that the Doppler method and spaced antenna method are, in fact, equivalent. Both techniques scatter from the same variations in the medium. Therefore, the effect of wave structures is equally a problem with the Doppler method and the SA method. There is no reason to expect that the latter will give poorer results on that account.

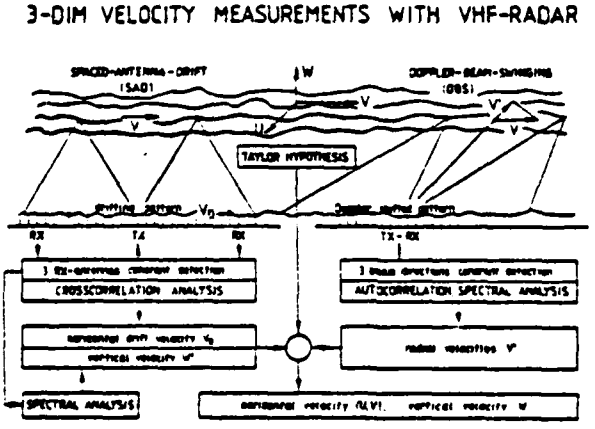

Figure 1. Schematic of the spaced antenna and the Doppler method for measuring the three-dimensional velocity in the troposphere, stratosphere, and mesosphere.

3. An experiment to compare the two techniques

The SOUSY-VHF-Radar is one of the few radars at present where a comparison between the Doppler technique and the spaced antenna technique can be carried out directly. The configuration of the antenna system is shown in Figure 2. The large antenna can be used for both transmitting and receiving in the Doppler mode. The three smaller antennas can also be used as spaced receivers in combination with the large transmitting array. In October 1979, an experiment was carried out with this radar to compare the two measurement techniques.

The spaced antenna wind measurements can be made either by cross-correlating

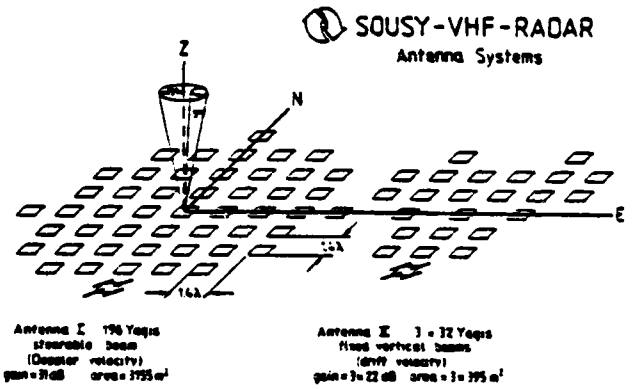

Figure 2. Antenna systems of the SOUSY-VHF-Radar (from Röttger 1981a). Antenna I is used in the Doppler mode for transmission and reception. Antenna II is the smaller system of 3 x 32 four-element Yagi antennas which are used in the spaced antenna mode for reception when the large array of 196 Yagis is used for transmission.

the received power at the three receiving antennas or by cross-correlating the complex amplitudes. The latter approach retains the phasing information and gives better results because it is consistent with the process of coherently integrating the signals. Figure 3 shows the resulting comparison. It is clear that the complex amplitude cross-correlation provides data over a greater height range than the simple power cross-correlation. Especially, the region between 8.2-km and 9.7-km altitude and the lower stratospheric heights should be compared.

It is well known that signals at VHF have a strong angular dependence near the zenith. Specular reflections or Fresnel scattering associated with the stable temperature stratification in the atmosphere produce enhanced echoes at vertical incidence. The echo strength decreases rapidly, by as much as 10 dB (Green and Gage, 1980), at even a few degrees off vertical. The spaced antenna technique makes maximum use of this effect since all the beams are pointed vertically, producing a higher

signal-to-noise ratio at those heights where the winds are measured. The Doppler method does not take advantage of the effect since the beams have to be pointed off vertical to make the wind measurements.

The strong angular dependence of the reflectivities does pose a potential problem for the Doppler technique when small antenna arrays are used. There are generally practical limitations on how far off vertical the beams can be pointed, and, of course, the beam width increases as the dimension of the antenna array decreases. When the beam width is wide, the received signal is really a convolution of the antenna pattern and the angular dependence of the echo strength, as shown in Figure 4. The result is that the apparent look angle is different than the real look angle, and the horizontal winds tend to be underestimated. The effect is critical when the vertical pointing direction is within the main lobe of the radiation pattern.

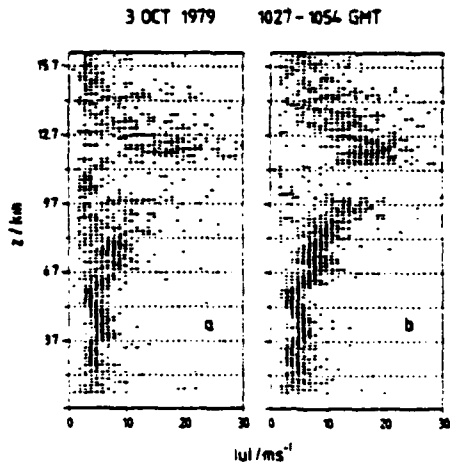

Figure 3. Height profiles of drift speed deduced from (a) power cross-correlation and (b) complex amplitude cross-correlation.

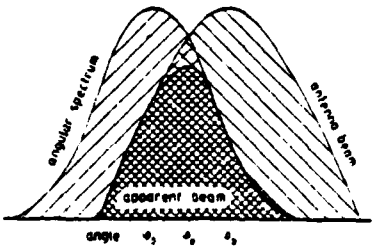

Figure 4. Formation of an apparent beam direction.

The effect is shown in the experimental results presented in Figure 5. Figure 5a shows the velocity profile derived from the complex crosscorrelation of the spaced antenna signals. Simultaneous aircraft wind measurements, shown by the open circles, indicate good agreement between the two independent wind measurements. Panel b shows the vertical velocity profile which could only be measured with the VHF radar.

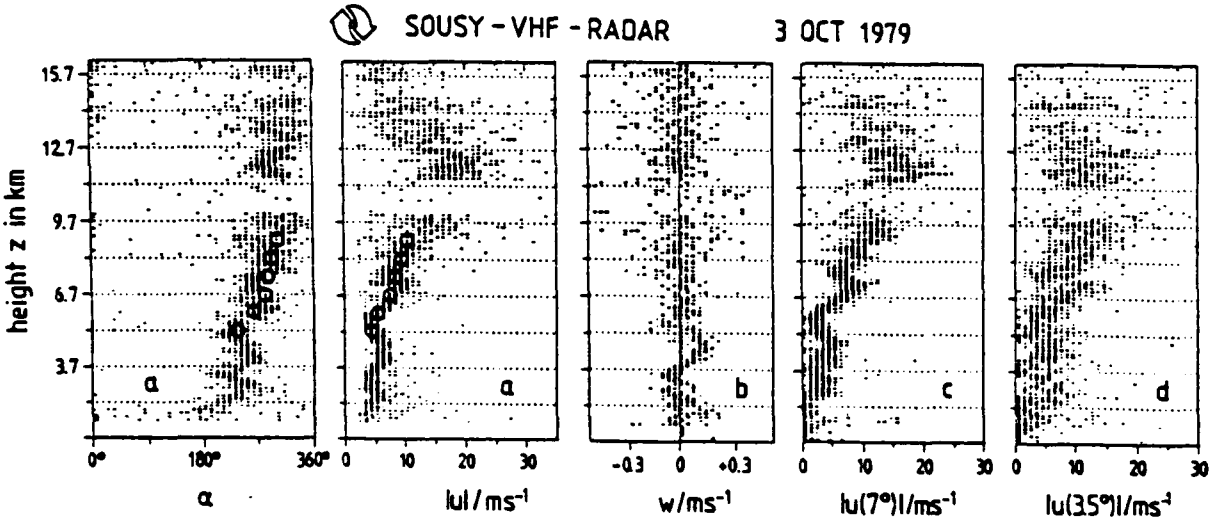

Figure 5. Height profiles of (a) wind direction and wind speed measured with the spaced antenna method and comparison with aircraft winds shown by the open circles, (b) vertical velocity, and (c) wind speed measured with the Doppler method using a beam pointing at 7° and (d) 3.5° off vertical.

Figure 5c gives the velocity profile derived from the Doppler method using a beam pointed 7° off vertical and shows very good agreement with the spaced antenna method. However, the beam width of the large array is 5°, and when the beam is pointed at only 3.5° off vertical, there is a significant contribution from the vertical direction. The resulting wind profile is much poorer since it has broader scatter and underestimates the velocities.

4. Discussion

The data from the October 1979 experiment are not conclusive, but they do indicate that there may be certain advantages in using the spaced antenna method, particularly for systems with small dimensions of the type likely to be used in operational wind profiling. Problems associated with aspect sensitivity only arise when the beam width is large. It is, in fact, likely that when larger systems are used, there is little difference between the two techniques since the beam widths are small then. Therefore, the SOUSY comparison may not fully show the advantages of the spaced

antenna method for small tropospheric sounding systems, and further comparisons should be carried out in the future.

REFERENCES

Briggs, B. H., 1980: Radar observations of atmospheric winds and turbulence: a comparison of techniques. J. Atmos. Terr. Phys., 42, 823-833.

Green, J. L., and K. S. Gage, 1980: Observations of stable layers in the troposphere and stratosphere using VHF radar. Radio Sci., 15, 395-406.

Larsen, M. F., 1983: The MST radar technique: Requirements for operational weather forecasting. Handbook for MAP, Workshop on Technical Aspects of MST Radar, University of Illinois, Urbana, in press.

Röttger, J., 1981a: Investigations of lower and middle atmosphere dynamics with spaced antenna drifts radars. J. Atmos. Terr. Phys., 43, 277-292.

Röttger, J., 1981b: The capabilities of VHF radars for meteorological observations. Proceedings, IAMAP Symposium on Nowcasting: Mesoscale Observations and Short-range Predictions, European Space Agency, Paris, SP-165.

Strauch, R. G., 1981: Radar measurement of tropospheric wind profiles. Preprints, 20th Conference on Radar Meteorology (Boston), AMS, Boston, pp. 430-434.

Strauch, R. G., M. T. Decker, D. C. Hogg, 1982: An automatic profiler of the troposphere. Preprints, AIAA 20th Aerospace Sciences Meeting (Orlando, Fla.), American Institute of Aeronautics and Astronautics, New York.

GEOPHYSICAL RESEARCH LETTERS, VOL. 10, NO. 4, PAGES 325-328, APRIL 1983

COMPARISON OF TROPOPAUSE HEIGHT AND FRONTAL BOUNDARY LOCATIONS BASED ON RADAR AND RADIOSONDE DATA

M.F. Larsen
School of Electrical Engineering, Cornell University, Ithaca, New York 14853

J. Röttger
EISCAT Scientific Association, Box 705, S-981 27 Kiruna, Sweden

Abstract. In February of 1982 the SOUSY-VHF-Radar, located near Hannover, West Germany, was operated during the passage of a warm front. The timing of the radiosonde ascent from nearby Hannover was such that the narrow frontal zone boundary was immediately overhead at a height of approximately 7 km. The data from this event has made it possible to make a detailed comparison of the radar and radiosonde reflectivity data that has not been possible before. We find that the frontal boundary that is detected by the radar appears as a very low tropopause height in the radiosonde data (approximately 3 km less than the mean during this time).

Introduction

Past studies of frontal zone dynamics have relied either on research aircraft (e.g., Danielsen, 1968; Shapiro, 1974, 1978, 1980, 1981; Shapiro and Kennedy, 1981) or cm-wavelength Doppler radar observations (e.g., Browning and Harrold, 1970; James and Browning, 1979; Hobbs and Biswas, 1979; Hobbs and Persson, 1982; Carbone, 1982) to resolve the small-scale features. Recently, a number of frontal passage observations have been made with the SOUSY-VHF-Radar located in the Harz Mountains near Hannover in West Germany (Röttger, 1979, 1981a,b; Röttger and Schmidt, 1981). The radar operates at a wavelength of 5.6 m and measures both the horizontal and vertical velocities directly overhead with a height resolution of 150 m and a time resolution of the order of a minute. Wind measurements are routinely available up to an altitude of almost 20 km. The SOUSY radar has a fixed dipole array constrained to look vertically and can obtain data either through the Spaced Antenna (SA) or Doppler Beam Swinging (DBS) method. The following data were obtained with the SA method. Thus, the radar can provide time/height cross sections, but it cannot measure horizontal variations directly as the aircraft and scanning radar can. However, the frontal-passage observations are unique because of the excellent spatial and temporal resolution, the height range covered, and because the radar can actually locate the frontal boundary as a band of increased echo strengths.

The reflectivity measured with a vertically beaming 6 m radar is particularly sensitive to inversions and other stratified temperature structure in the atmosphere (Green and Gage, 1980; Rastogi and Röttger, 1982). Wavelengths in the range from 1 to 10 cm that have been used for meteorological radars traditionally are also sensitive to such structure to some extent (see e.g., Atlas et al., 1966), but the effect is much greater at frequencies in the VHF range. Also, the longer wavelength is much less sensitive to echoes from precipitation than wavelengths in the centimeter range.

In February of 1982 a cold front and a warm front passed the location of the SOUSY radar, and data were taken over a period of several days both preceding and following the frontal passage. This particular event was unique because the radiosonde ascent from nearby Hannover occurred so that the radiosonde passed directly through the frontal boundary during the ascent. The boundary is a very narrow feature of small horizontal extent in the direction parallel to the direction of movement of the front. In the February event, the traversal time of the frontal boundary was between 2 and 6 hours, dependent on altitude. Typically, the radiosonde ascents will miss the boundary since successive launches are separated by 12 hours. The timing in this particular event was fortuitous, and the comparisons between the radar and radiosonde data show good agreement. We will concentrate on a comparison of the radar reflectivity data and the reflectivity calculated from the nearby Hannover radiosonde data.

Synoptic Situation

On February 7, 1982 a secondary low-pressure center formed along a long occluded frontal boundary associated with a low centered over Iceland. The new low became identifiable approximately 200 km west of Brest, France at 12Z on February 7 (Deutscher Wetterdienst, 1982a,b). By this time both the warm and cold front were identifiable at the surface, though the horizontal temperature gradients were weak. The 300-mb and 500-mb upper air charts showed a cutoff low 15° due west of Morocco. At 12Z a short wave with main axis running from northwest to southeast between 40°N and 50°N was deepening at 300-mb as the trough axis aligned with the cutoff low. During the next 24 hours, the short wave had moved approximately 20° in longitude further eastward, and the wave axis lay along the western coast of France. By 00Z on February 9, significant amplification had taken place, and a cutoff high had formed over the Bay of Biscay. The winds aloft over Central Europe had changed direction from essentially zonal to a strong northerly flow.

Figure 1 shows the time height cross section of temperature as measured by the Han-

Paper number 3L0304.
0094-8276/83/003L-0304$3.00

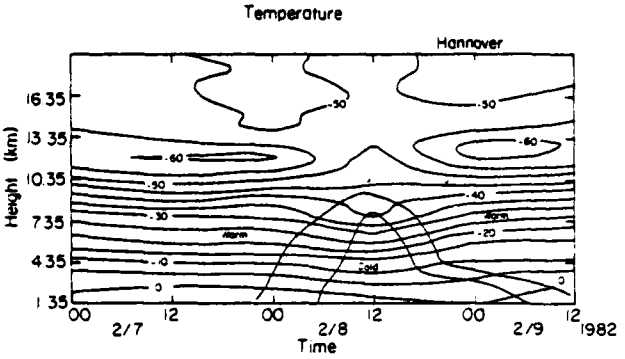

Fig. 1. Time/height cross-section of temperature from the Hannover radiosonde station. Heavy solid lines show the boundaries between warm and cold air. The J's show the location of the jets as determined from the radar wind measurements.

nover radiosonde. Regions of warm and cold air have been labeled, and the locations of the fronts separating the different air masses are indicated. Both fronts are fairly weak, but the warm front is narrower in horizontal extent than the cold front. The position of the two jets, indicated by "J's", was determined from the radar wind measurements that will be presented in more detail in a later paper.

Radar Data

Radar data are available for the period beginning at 00Z on February 6 and ending at 00Z on February 11. The radar measures signals caused by partial reflections from turbulence induced structures in the refractive index. One large transmitting antenna was used. To measure horizontal winds three separate arrays were used to receive the signals, and the horizontal winds were calculated from the cross-correlation between the echoes received at each array. The vertical winds were measured directly from the Doppler shift of the echoes. The echo power is the third parameter measured by the radar, and it is converted into relative radar reflectivity by correcting for the r^2 dependence. The technique is described by Röttger (1981c).

During the period discussed here, measurements were made for 4 min every hour on the hour. All data presented are an average value for the corresponding 4-min period. This particular sampling scheme was used to reduce the amount of raw data that had to be processed to one tape per 24 hours. At the present time only preintegration, but no further preprocessing, of the received signals is done on line.

The height range in which there is a usable signal stretches from the lower limit of 1.35 km MSL, 900 m above the radar, to a maximum of approximately 20 km. The lower limit is set by the receiver recovery time, ground clutter, and atenna near-field effects. The upper limit is determined by the decreasing signal-to-noise ratio obtained with the applied average transmitter power of 20 KW, the effective antenna aperture of 2500 m^2, and the given range resolution of 150 m.

Reflectivity Data

The reflectivities measured with the VHF radar as a function of time and height are shown in Figure 2. The increment between contours is 3 dB, and the regions of stronger echoes have been shaded. A band of higher reflectivities is evident above 11 or 12 km in the vicinity of the tropopause. Long-wavelength radars are extremely sensitive to stratification in the temperature structure of the atmosphere, and it has been shown by Röttger (1980) and Green and Gage (1980) that radars operating in the VHF regime can be used to determine the height of the tropopause. The radiosonde station located closest to the SOUSY site is Hannover, 100 km northwest. The tropopause heights determined from the radiosonde data at the standard 12-hour intervals have been plotted in Figure 2 as the heavy crosses. There is good agreement between the radar and radiosonde observations taking into account that the radar sees the "radar" tropopause which is a few hundred meters above the meteorological tropopause (Rastogi and Röttger, 1982).

At 12Z on February 8, a band of strong reflectivities stretches downward from the tropopause and merges with the region of strong echoes below 7 km. The band coincides with the location of the warm front shown in Figure 1. The cold front does not show up as clearly, but if the shading threshold is decreased by 6 dB, as shown by the cross-hatched area in Figure 1, the structure associated with the cold front begins to emerge. Presumably the 4-min sampling period is too short to smooth out the short term fluctuations of the weaker signals from the cold frontal boundary. The radar is able to detect the frontal surface for the same reason that it can detect the lower edge of the tropopause boundary. The temperature stratification associated with the front enhances the echoes at long wavelengths. This type of structure has been observed consistently with the radar during a number of other warm frontal passages. In this particular case we have much more detailed corroboration from the independent radiosonde measurements, showing that the structure is real. Figure 2 shows that the

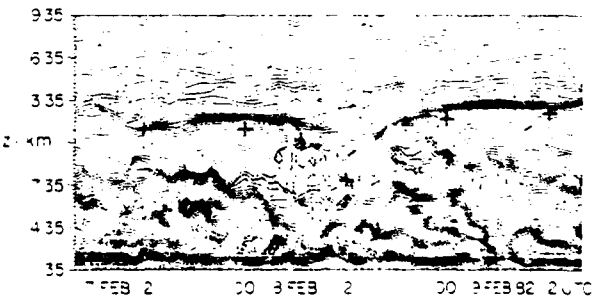

Fig. 2. Time/height cross-section of the reflectivities measured by the SOUSY-VHF-Radar. The contour interval is 3 dB. Regions of highest echo intensity have been stippled. The cross-hatched areas show echoes that are within 6 dB of the echo strengths in the stippled areas.

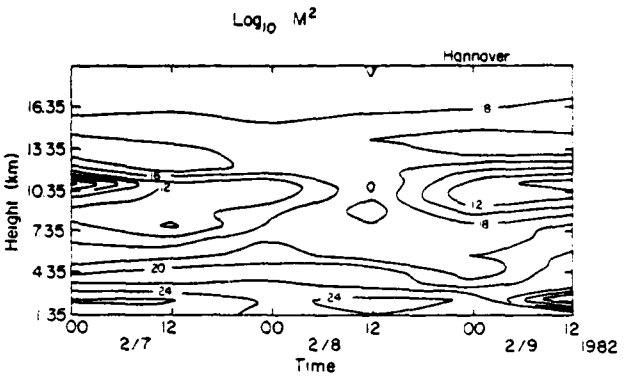

Fig. 3. Logarithm of the vertical gradient of the potential refractive index calculated from the Hannover radiosonde data.

frontal boundary, i.e., the boundary between the stippled and nonstippled area, is extremely narrow in time and therefore, we deduce, also in the horizontal direction. The twelve hour interval between successive balloon launches makes it difficult to observe with the conventional meteorological observing network. However, in this case the boundary passage coincided with the balloon launch at 12Z. The tropopause height reported by Hannover at that time was extremely low but in agreement with the radar data, giving a strong indication that the band of higher radar reflectivities really shows the position of the front.

The radar reflectivities are proportional to M^2 with M given by (Ottersten, 1969)

$$M = -77.6 \times 10^{-6} \frac{P}{T} \left(\frac{\partial \ln \theta}{\partial z}\right) \cdot \left\{ 1 + \frac{15500q}{T} \left(1 - \frac{1}{2} \frac{\partial \ln q / \partial z}{\partial \ln \theta / \partial z}\right) \right\}$$

Here M is the mean vertical gradient of the potential refractive index, P is pressure, T is temperature, q is the specific humidity, and θ is the potential temperature. The radiosonde data from Hannover were used to calculate the reflectivities using the above formula, and the results are plotted in Figure 3. The contour interval is 3 dB. The same features are evident in both Figures 2 and 3, though the measured radar reflectivities show more of the detailed structure since the time resolution is more than a factor of ten better.

Conclusion

The data presented here have shown that the radar can detect the warm frontal boundary even when the temperature gradients are relatively weak. In general there is a great potential for using sensitive radars like the SOUSY-VHF-Radar for studies of synoptic and mesoscale interactions. The high time and spatial resolution that can be achieved routinely with such an instrument and the relatively low cost of operation once the initial investment for construction of the radar facility has been covered are two features of this measurement technique that cannot be rivaled by other techniques. Larsen and Röttger (1982) have discussed the applications of the radars to meteorological research in greater detail.

Acknowledgments. The assistance of staff members of the Max-Planck-Institut is gratefully acknowledged, particularly G. Monecke. The authors are thankful for the support of the Deutscher Wetterdienst in providing the surface and upper air charts, and the radiosonde data. MFL was supported by the Air Force Office of Scientific Research under grant AFOSR-80-0020 during the course of this study.

References

Atlas, K., K. R. Hardy, K. M. Glover, I. Katz, and T. G. Konrad, Tropopause detected by radar, Science, 153, 1110-1112, 1966.

Balsley, B. B., and K. S. Gage, On the use of radars for operational wind profiling, Bull. Amer. Met. Soc., 63, 1009-1018, 1982.

Browning, K. A., and T. W. Harrold, Air motion and precipitation growth at a cold front, Quart. J. Roy. Meteor. Soc., 96, 369-389, 1970.

Carbone, R. E., A severe frontal rainband. Part I: Stormwide hydrodynamic structure, J. Atmos. Sci., 39, 258-279, 1982.

Danielsen, E. F., Stratospheric-tropospheric exchange based on radioactivity, ozone, and potential vorticity, J. Atmos. Sci., 25, 502-518, 1968.

Deutscher Wetterdienst, Wetterkarte des Deutschen Wetterdienstes, Deutscher Wetterdienst, Seewetteramt, Hamburg, 1982a.

Deutscher Wetterdienst, Europaischer Wetterbericht, Deutscher Wetterdienst, Zentralamt, Offenbach, 1982b.

Green, J. L., and K. S. Gage, Observations of stable layers in the troposphere and stratosphere using VHF radar, Radio Sci., 15, 395-406, 1980.

Hobbs, P. V., and K. R. Biswas, The cellular structure of narrow cold-frontal rainbands, Quart. J. Roy. Meteor. Soc., 105, 723-727, 1979.

Hobbs, P. V., and P. O. G. Persson, The mesoscale and microscale structure and organization of clouds and precipitation in midlatitude cyclones. Part V: The substructure of narrow cold-frontal rainbands, J. Atmos. Sci., 39, 280-295, 1982.

James, P. K., and K. A. Browning, Mesoscale structure of line convection at surface cold fronts, Quart. J. Roy. Meteor. Soc., 105, 371-382, 1979.

Larsen, M. F., and J. Röttger, VHF and UHF Doppler radars as tools for synoptic meteorology, Bull. Amer. Met. Soc., 63, 996-1008, 1982.

Ottersten, H., Mean vertical gradient of potential refractive index in turbulent mixing and radar detection of CAT, Radio Sci., 4, 1247-1249, 1969.

Rastogi, P. K., and J. Röttger, VHF radar observations of coherent reflections in the vicinity of the tropopause, J. Atmos. Terr. Phys., 44, 461-469, 1982.

Röttger, J., VHF radar observations of a frontal passage, J. Appl. Meteor., 18, 85-91, 1979.

Röttger, J., Structure and dynamics of the stratosphere and mesosphere revealed by VHF radar investigations, Pure Appl. Geophys., 118, 494-527, 1980.

Röttger, J., The capabilities of VHF radars for meteorological observations, in Nowcasting: Mesoscale Observations and Short-Range Prediction, European Space Agency, Paris, 1981a.

Röttger, J., Wind variability in the stratosphere deduced from spaced antenna VHF radar measurements, Preprint Volume, 20th Conference on Radar Meteorology, Nov. 30-Dec. 3, 1981, (Boston), AMS, Boston, Mass., 1981b.

Röttger, J., Investigations of lower and middle atmosphere dynamics with spaced antenna drifts, J. Atmos. Terr. Phys., 43, 277-292, 1981c.

Röttger, J., and G. Schmidt, Characteristics of frontal zones determined from spaced antenna VHF radar observations, Preprint Volume, 20th Conference on Radar Meteorology, Nov. 30-Dec. 3, 1981 (Boston), AMS, Boston, Mass., 1981.

Shapiro, M. A., A multiple structured frontal zone-jet stream system as revealed by meteorologically instrumented aircraft, Mon. Wea. Rev., 102, 244-253, 1974.

Shapiro, M. A., Further evidence of the mesoscale and turbulent structure of upper level jet stream-frontal zone systems, Mon. Wea. Rev., 106, 1100-1111, 1978.

Shapiro, M. A., Turbulent mixing within tropopause folds as a mechanism for the exchange of chemical constituents between the stratosphere and troposphere, J. Atmos. Sci., 37, 994-1004, 1980.

Shapiro, M. A., Frontogenesis and geostrophically forced secondary circulations in the vicinity of jet stream-frontal zone systems, J. Atmos. Sci., 38, 954-973, 1981.

Shapiro, M. A., and P. J. Kennedy, Research aircraft measurements of jet stream geostrophic and ageostrophic winds, J. Atmos. Sci., 38, 2642-2652, 1981.

(Received December 20, 1982;
accepted February 1, 1983.)

Invited review: Proceedings of the SCOSTEP/ URSI/MAP Workshop on Technical Aspects of MST Radar, May 23-27, 1983, Handbook for MAP series, University of Illinois, Urbana, Illinois, 1983.

The MST Radar Technique:

Requirements for Operational Weather Forecasting

Miguel Folkmar Larsen
School of Electrical Engineering
Cornell University
Ithaca, NY 14853

1. Introduction

Recent interest in improving our ability to make mesoscale forecasts has been the result of improving observational technology and theoretical understanding of mesoscale motions. There is a feeling that the accuracy of forecasts for spatial scales of less than 1000 km and time scales of less than 12 hours can be improved significantly if our resources are applied to the problem in an intensive effort over the next decade. Since the most dangerous and damaging types of weather occur at these scales, there are major advantages to be gained if such a program is successful. The interest in improving short term forecasting is evident in the series of papers resulting from the International IAMAP Symposium on Nowcasting [Browning, 1982], the paper on the long-term goals of NOAA as presented by Schmidt [1983] at the Fifth Symposium on Meteorological Observations and Instrumentation, and the two handbooks published by the UCAR committee on the National STORM (Stormscale Operational and Research Meteorology) Program [UCAR, 1982; Anthes, 1983]. The conclusion of all of these publications is that the technology at the present time is sufficiently developed, both in terms of new observing systems and the computing power to handle the observations, to warrant an intensive effort to improve stormscale forecasting.

The National STORM Program handbooks [UCAR, 1982, Anthes, 1983] are excellent source books on the general problem of short term forecasting. The

first handbook summarizes the need for this type of forecasting and the framework for achieving the desired improvements. The second handbook gives a detailed assessment of our capabilities and understanding at the present and the areas of research most in need of attention. Questions that will have to be addressed deal with the type of observing system or systems that will be used to generate data compatible with the scales of motion being discussed and the way the data will be used operationally. Hooke [1983] summarized the situation as follows:

> Within the next several years, operational meteorology will be facing some crucial decisions regarding measurement systems. The most obvious and important example is the determination of winds. A variety of remote sensing techniques have been used experimentally to measure wind direction and speed in clear air. There is substantial need for an integrated effort to determine which of these techniques is most promising by testing alternative methods in the field. This will be a necessary prelude to the procurement and deployment of a next-generation wind sensing system.

In this review I will attempt to provide an assessment of the extent to which the so-called MST radar technique fulfills the requirements for an operational mesoscale observing network, and I will delineate the extent to which improvements in various types of forecasting could be expected if such a network is put into operation.

2. Characteristics and capabilities of the radar technique

The MST radar measures the vertical profile of horizontal winds based

either on the Doppler shift of the signal backscattered from turbulent variations in the refractive index or from the cross-correlation between the signals received at a set of three spaced antennas. The technique has been described in detail by Woodman and Guillen [1974], Gage and Balsley [1978], Balsley and Gage [1980], and Rottger [1980] among others. Details and advantages of various specific measurement techniques are discussed in much greater detail in other papers in this volume.

I will concentrate on VHF radars that use a fixed dipole array and are capable of measuring the vertical profile of the horizontal winds as a minimum. Some MST radars operating at shorter wavelengths have fully steerable dishes. An example is the 23 cm radar formerly located at Chatanika, Alaska, and now located in Søndre Strømfjord, Greenland. I will not consider such radars here since they are in the same category as the existing weather radar network if upgraded to provide Doppler capability.

The radar's ability to provide wind profiles is something that is duplicated by the standard rawinsonde. However, the radar wind measurements have many advantages, particularly if the mesoscale is of interest. The radar wind profiles can be measured as often as desired down to the imposed equipment limitation of a few minutes. There are no expendables involved except for the power used to run the radar equipment. Also, the radar measures the wind profile immediately above the radar. During periods of high winds, the rawinsonde can drift as much as 100 km during its ascent. Such an error can be a major one if the scales of motion of interest are of the order of a few hundred kilometers. Finally, a large part of the cost of running a radiosonde station has always been the salaries of the personnel. Since the radar measurements are easily automated, adding VHF Doppler radars to the network

would only increase the required extra manpower by a small fraction of the number of personnel needed if an equal number of new radiosonde stations were established. The success of such an approach is already evidenced by the Poker Flat MST Radar which has been operating unattended since 1979.

However, the comparison between the radiosonde and the radar is not really the most appropriate. The possibility of establishing a mesoscale radiosonde observing network has never been considered very seriously since the cost is prohibitive. Most likely the competition will come from satellites or some other ground-based remote sensing system such as sodars or lidars. The primary advantage of the radar over the acoustic sounder is the height range covered and the insensitivity of the former to various forms of noise. A very complete review of the capabilities of the acoustic sounding technique is given by Brown and Hall [1978]. The lidar is competitive with the radar in terms of the height range covered and the time and, certainly, the height resolution, but the lidar is seriously hampered when there is precipitation or fog or simply when it is overcast [Strauch and Cohen, 1972]. The lidar provides information on atmospheric density and humidity, but the radar provides data on the height of the tropopause and other temperature structure such as inversions and fronts. Further comparison between the advantages of the two techniques is needed, although the main drawback of the lidar for operational applications appears to be the limitations of the technique when used in the presence of clouds.

The satellite has a number of advantages over the radar. Primarily it provides vast areal coverage in relatively short periods of time. Since a very large source of error for large scale forecasting is due to a lack of data in sparsely populated regions, underdeveloped areas, and the oceans, satellite

measurements appear to be the best hope for improving large-scale observations. The radars do not immediately offer any hope for providing data in data sparse regions. The height and time resolution, and the height range covered by the radar is significantly better than that of the satellite, but the lack of spatial coverage of the radar measurement is still one of the limitations of the technique.

So far, I have compared the advantages and disadvantages of the various techniques. It is clear that the radar by itself cannot replace the other types of measurements, but it can provide a relatively inexpensive solution to the problem of upgrading the observing network to provide mesoscale resolution. Meteorological radars already exist and provide important information for the forecaster. Half-hourly satellite photos are an important input to the forecast process and satellite measurements of temperature and winds are providing data for areas where no information could be obtained otherwise, albeit with less than desirable height resolution. However, the VHF radars can fill the gaps that exist in the present radiosonde network. It has been shown by Hoke and Anthes [1976], Daley and Puri [1980], and Daley [1980] among others that when small scales of motion are of interest, the wind information is more important than pressure and temperature information. Therefore, the fact that the radar only measures the winds, and not also pressure and temperature, should not necessarily be viewed as a compromise of the technique when it is used for mesoscale observations. I will discuss this point in more detail in Section 5.

3. Requirements for an operational system

Although the topic of the workshop is the MST (Mesosphere-Stratosphere-Troposphere) radar, the ability to measure winds in

the troposphere, stratosphere, and mesosphere is not required of the systems used for mesoscale weather forecasting. A simple "Model T" Radar would be sufficient. With thanks to Henry Ford, such a radar should be simple to mass produce, low cost, and dependable in operation. The reductions in antenna size and transmitter power gained by reducing the design specifications of the system could reduce the cost of the system by as much as a factor of ten when compared to an MST system. That is a crude estimate but probably not unrealistic.

Discussions about the applicability of the radar wind measurements to operational weather forecasting have generally centered on applications to large-scale forecasting with improved spatial resolution so that mesoscale phenomena can be resolved. Of course, it is important that this aspect of the radar technique should be discussed, and that may be how the systems are ultimately applied. However, there are intermediate applications for such systems that would allow the radars to be phased into the large-scale observing network with possible significant forecast improvements at each intermediate step. There are a number of very localized phenomena that lead to severe weather that a small network of VHF radars could be useful in forecasting.

Applications that come to mind include the following. A network of between 3 and 6 radars distributed around the Great Lakes could be used for operational forecasting of lake-effect snows. Typically, the snows are generated by directional changes in the mesoscale flow patterns and eventually mesoscale circulations develop in response to the heating effects of the lakes [Zipser, 1983]. It should be possible to detect these small scale circulation changes with a network of radars. More study would be needed to determine the real usefulness of such a system for forecasting this very specific local

phenomenon.

A second application would involve use of a system of radars as a forecast tool for the severe Colorado wind storms that occur everyyyear in the lee of the Rocky Mountains [Lilly and Zipser, 1972; Klemp and Lilly, 1975]. Since a cloudy or precipitating atmosphere is not necessarily associated with this phenomena, a scanning weather radar, even one with Doppler capability, is not particularly useful for forecasting this type of event. Actually, the necessary network may already exist in the form of the PROFS (Prototype Regional Observing and Forecasting System) network of wind profilers operated by the Wave Propagation Laboratory of NOAA [Strauch et al., 1982].

Another application of a small-scale system of Model T radars is for studies of the sea breeze in the Florida peninsula. The sea breeze develops in response to the diurnal heating cycle and the temperature differences between land and sea. The vertical circulation that develops acts as a modulator of the convective activity over the land and over the ocean [Lhermitte and Gilet, 1975; Atkinson, 1981]. The resulting thunderstorms can be very severe and may involve large shears, heavy rainfall rates, hail, and turbulence that can be a hazard to local aviation. A scanning weather radar can be used to detect the developing cells, but since the lifetime of a single cell is from 30 to 45 minutes, only a short term warning can be issued. Clear air wind measurements may be capable of detecting the buildup of the conditions leading to intense convection.

The possible applications of the radar systems for local forecasting just named are only a few of the possibilities. The important point is that a small number of the radar systems can be installed to provide improved forecasting of specific local phenomena. Confidence in the systems and operational experience

would be gained before making a commitment to use the radars on a networkwide basis.

Another area in which the radars can be applied for forecasting purposes relates to pollutant dispersion. Most of the models used to estimate dispersion of pollutants are based on the Gaussian plume models [Hanna et al., 1982]. The two major input parameters are an atmospheric stability index derived from the radiosonde temperature profile and the wind at the height of the center of the plume. A major problem is the significant diurnal variation in the winds that cannot be resolved by the rawinsonde measurements made once every 12 hours [Draxler, 1983]. Only a small system that could measure the winds up to a height of a few kilometers would be needed to improve the wind information data base significantly. Other locations that could benefit from such a system would be airports where the primary hazard is from clear air turbulence and downdrafts that affect aircraft during takeoff and landings. Again only measurements within the boundary layer or a little higher would be required. There are no doubt other possibilities.

4. Previous work

Very little work has been done to date dealing directly with applicability of the radars to the forecasting problem. Balsley and Gage [1982] have discussed considerations for implementation of an operational radar system including antenna size needed, most favorable frequency ranges, and the type of power needed. Carlson and Sundararaman [1982] have made a preliminary case showing that a few percent of the annual fuel consumption of the airlines could be saved if data from a wind measuring radar network was available for flight planning purposes. They indicate that a detailed study has to be made to determine if their rough calculations of potential savings are correct.

However, the savings that they envision would be enough to justify the cost of a radar network within the first year.

Fukao et al. [1982] have made a detailed comparison of rawinsonde data from San Juan, Puerto Rico and wind profiles measured with the Arecibo 430 MHz radar. Twenty-six separate days from August and September of 1977 were involved in the study. The comparison indicated a difference of 4.9 m/s in the upper troposphere and a difference of 3.3 m/s in the lower stratosphere. The difference in the lower stratosphere could be explained by the experimental error in the rawinsonde measurement, but the larger difference in the upper troposphere was apparently due to spatial variations over the 80 km distance separating the two sites.

Larsen [1983] investigated the effect of high frequency meteorological noise on the representativeness of the radar wind data. *If one is interested* in using the data for input to a numerical model that can resolve synoptic and mesoscale motions down to scales of a few hundred kilometers, any motions with smaller scales are effectively just noise or an error in the measurement. The radar wind measurements from the Poker Flat MST radar were compared to the rawinsonde measurements from Fairbanks, Alaska, and both were compared to the geostrophic wind calculated by applying an objective analysis scheme to the standard radiosonde data from five nearby stations. By averaging the high time resolution radar data over intervals of several hours, the high frequency oscillations could be filtered out. The comparison showed that the radar and rawinsonde data agreed to within 2-3 m/s when the radar data was averaged over 12 hours or more, and that the difference between the radar winds and the geostrophic winds was about the same as the difference between the rawinsonde winds and the geostrophic wind. The two independent wind measurements were

most similar, and both differed from the geostrophic wind by 1.5-2.0 m/s more than they differed from each other. The results indicate that it is crucial that the data should be averaged in some way if it is used as input to a numerical model. The errors decrease as the averaging interval is increased. Therefore, the acceptable error for a given model will have to be determined in order to know how to process the radar data.

Larsen and Rottger [1983] have shown that a VHF radar can detect the location of frontal boundary surfaces as enhancements of the radar reflectivity. When coupled to the measurements of the horizontal and vertical wind components, such information would be of value in forecasting the development and position of fronts since such small-scale features are not resolved by the synoptic observing system or in operational numerical forecast models.

Green et al. [1978] showed the ability of the radar to detect changes in the jet stream height and intensity in real time, as well as gravity wave activity and vertical velocities associated with the jet stream. Turbulence intensity and location can also be determined along with the rate of turbulent dissipation [Gage et al., 1978]. The results are intriguing, and more work needs to be done in this area. One very interesting aspect of their study is that radar measurements may be used in the future to provide real time inputs for the parameterization schemes used in numerical models. All processes in a numerical model with spatial scales smaller than the models grid spacing are parameterized. Such things as the vertical fluxes of heat and momentum due to convection and the loss of energy to subgrid scales are included in the parameterizations. The schemes used usually depend in some way on the physical quantities calculated by the model, but the high time resolution measurements

of the radar, along with the vertical velocity measurements [e.g., Ecklund et al., 1982], may provide valuable information on the actual magnitude of these various quantities as a function of time and location.

The most detailed investigation of the applicability of the radar technique to mesoscale forecasting is being undertaken by the Wave Propagation Laboratory of NOAA using their Profiler system [Strauch, 1981; Strauch et al., 1982]. The Profiler uses several microwave radiometers to measure the temperature and humidity profile. A set of three Doppler radars distributed in a triangular network around Boulder, Colorado is used to resolve mesoscale features in the local winds. The system is dedicated to the problem of mesoscale forecasting. Except for results dealing with the measurement capabilities of the system and the corresponding accuracies, few results are available to date. However, the Profiler should provide a good assessment of potential improvements in mesoscale forecasting that can be realized with such a system.

5. Optimal specification of initial data

Much of the discussion about using the MST systems operationally has focused on the WPL Profiler which uses a clear air radar for wind profiling. However, the system was designed to test the possibility of replacing the standard National Weather Service radiosonde. To this end, microwave radiometers are used to provide profiles of the temperature and humidity, though to date the achievable height resolution has been less than that of the radiosonde. It remains to be seen whether the difference is significant.

There is little doubt that the thermodynamic and moisture information is valuable, but in this case we should question whether the extra cost would be justified on a networkwide basis. The radiometers are by far the most

expensive part of the system. The cost ratio between the Model T radar discussed here and the microwave system may be as great as 1 to 5 for an operational system. The estimated cost of a Profiler system has been given as approximately $500,000 [Decker, 1983]. Carlson and Sundararaman [1982] estimate that a tropospheric wind profiling system, without the radiometers, could be built for 10% of that sum or less.

Will the wind information be useful in and of itself? The answer apparently is yes. Studies by Rutherford and Asselin [1972], Williamson and Dickinson [1972], Hoke and Anthes [1976], Daley and Puri [1980], Daley [1980], and Bube and Ghil [1982] indicate that at small scales the wind information is by far the most important. Small scales in this case are defined by a horizontal scale related to the Rossby radius of deformation. The various studies have used either analytic models or numerical models that characterize the dynamics of the atmosphere and considered the problem of how new information is assimilated into the model. The winds and the thermodynamic variables have been given as initial conditions singly and in combination. Updating the calculated fields with the pressure fields would eventually cause an adjustment to the input data, but the adjustment time would be long. However, the wind information is readily absorbed with a minimum of wave noise being generated. The pressure field then adjusts to reflect the changes in the wind field so that a complete set of information relevant to the small-scale motions is obtained even though only the wind fields are used as input. There seems to be agreement that wind information is more important for scales less than 1000-2000 km. At large scales the reverse is true, and the thermodynamic information is more important.

The physical reason for this effect is associated with the process known

as geostrophic adjustment and first described by Rossby [1938]. The crucial parameter in the problem is the Rossby radius of deformation given by the ratio of the speed of sound, or the propagation velocity of gravity waves of the appropriate scale, to the Coriolis parameter [Blumen, 1972]. At scales much larger than the Rossby radius, the wind field will adjust to balance a perturbed pressure field. For scales smaller than the Rossby radius, the pressure field adjusts to balance the wind field. Therefore, the smaller the scale of motion that is of interest, the more useful is the wind information. Since the mesoscale lies in the range of spatial scales where the wind information is most useful, there may be a significant improvement in our ability to forecast for this scale even if only the wind fields are measured. Shapiro et al. [1983] also discussed the importance of wind information at small scales, and they indicate that improved spatial resolution may be obtained from the measurements of a single radar if the data are used to extrapolate quantities along air parcel trajectories.

6. Conclusion

This article was meant to suggest a number of possible applications for the MST radar technique in operational weather forecasting. The results to date have shown that there is great promise for the technique as part of the standard observing network once it is resolved to increase the resolution to include mesoscale motions. In reality, very little work has been done to date relating to the forecast improvements that actually can be achieved with an operational wind profiling system. Forecast improvements due to a network of radars should be investigated both theoretically and experimentally. The possibility of using the radar data to refine some of the parameterization schemes used in forecast modeling should also be investigated. Finally, the

applications of the radar systems to forecasting area-specific phenomena should be examined in the near future.

REFERENCES

Anthes, R. A., The National STORM Program: Scientific and Technological Bases and Major Objectives, University Corporation for Atmospheric Research, Boulder, Colorado, 1983.

Atkinson, B. W., Meso-scale Atmospheric Circulations, Academic Press, New York, 1981.

Balsley, B. B., and K. S. Gage, The MST radar technique: Potential for middle atmospheric studies, Pure Appl. Geophys., 118, 452-493, 1980.

Balsley, B. B., and K. S. Gage, On the use of radars for operational wind profiling, Bull. Amer. Meteor. Soc., 63, 1009-1018, 1982.

Blumen, W., Geostrophic adjustment, Rev. Geophys. Space Phys., 10, 485-528, 1972.

Brown, E. H., and F. F. Hall, Jr., Advances in atmospheric acoustics, Rev. Geophys. Space Phys., 16, 47-110, 1978.

Browning, K. A. (ed.), Nowcasting, Academic Press, New York, 1982.

Bube, K. P., and M. Ghil, Assimilation of asynoptic data and the initialization problem, in Dynamic Meteorology: Data Assimilation Methods, L. Bengtsson, M. Ghil, and H. Kallen, eds., Applied Mathematical Sciences Series, Vol. 36, Springer-Verlag, New York, 1982.

Carlson, H. C., Jr. and N. Sundararaman, Real-time jetstream tracking: National benefit from an ST radar network for measuring atmospheric motions, Bull. Amer. Meteor. Soc., 63, 1019-1026, 1982.

Daley, R., On the optimal specification of the initial state for deterministic forecasting, Mon. Wea. Rev., 108, 1719-1735, 1980.

Daley, R., and K. Puri, Four-dimensional data assimilation and the slow manifold, Mon. Wea. Rev., 108, 85-99, 1980.

Draxler, R. R., Variability in winds and temperatures from sequential rawinsonde ascents, Preprint Volume, Fifth Symposium on Meteorological Observations and Instrumentation, April 11-15, 1983, Toronto, Ont., Can., AMS, Boston, Mass., 1983.

Ecklund, W. L., K. S. Gage, B. B. Balsley, R. G. Strauch, and J. L. Gree, Vertical wind variability observed by VHF radar in the lee of the Colorado Rockies, Mon. Wea. Rev., 110, 1451-1457, 1982.

Fukao, S., T. Sato, N. Yamasaki, R. M. Harper, and S. Kato, Winds measured by a UHF Doppler radar and rawinsondes: Comparisons made on twenty-six days (August-September 1977) at Arecibo, Puerto Rico, J. Appl. Met., 21, 1357-1363, 1982.

Gage, K. S., and B. B. Balsley, Doppler radar probing of the clear atmosphere, Bull. Amer. Meteor. Soc., 58, 1074-1093, 1978.

Gage, K. S., J. L. Green, and T. E. VanZandt, Application of the VHF pulsed Doppler radar to cloud physics research, Preprint Volume, Conference on Cloud Physics and Atmospheric Electricity, July 31-August 4, 1978, Issaquah, Washington, AMS, Boston, Mass., 1978.

Green, J. L., K. S. Gage, and T. E. VanZandt, Three dimensional observations of a jet stream using a VHF Doppler radar, Preprint Volume, 18th Conference on Radar Meteorology, March 28-31, 1978, Atlanta, Georgia, AMS, Boston, Mass., 1978.

Hanna, S. R., G. A. Briggs, and R. P. Hosker, Jr., Atmospheric Diffusion, National Technical Information Service, Springfield, Virginia, 1982.

Hoke, J. E., and R. A. Anthes, The initialization of numerical models by a

dynamic-initialization technique, Mon. Wea. Rev., 104, 1551-1556, 1976.

Hooke, W., Observation and data assimilation: Present status and future research-and-development opportunities, in The National STORM Program: Scientific and Technological Bases and Major Objectives, R. A. Anthes (ed.), University Corporation for Atmospheric Research, Boulder, Colorado, 1983.

Klemp, J. B., and D. K. Lilly, The dynamics of wave-induced downslope winds, J. Atmos. Sci., 32, 320-339, 1975.

Larsen, M. F., Can a VHF Doppler radar provide synoptic wind data?: A comparison of 30 days of radar and radiosonde data, Mon. Wea. Rev., in press, 1983.

Larsen, M. F., and J. Rottger, VHF and UHF Doppler radars as tools for synoptic research, Bull. Amer. Meteor. Soc., 63, 996-1008, 1982.

Lhermitte, J. S., and M. Gilet, Dual-Doppler radar observation and study of sea-breeze convective storm development, J. Appl. Met., 14, 1346-1361, 1975.

Lilly, D. K., and E. J. Zipser, The front range windstorm of 11 January 1972 -- A meteorological narrative, Weatherwise, 25, 56-63, 1972.

Rossby, C.-G., On the mutual adjustment of pressure and velocity distributions in certain simple current systems, 2, J. Mar. Res., 1, 239-263, 1938.

Rottger, J., Structure and dynamics of the stratosphere and mesosphere revealed by VHF radar investigations, Pure Appl. Geophys., 113, 494-527, 1980.

Rutherford, I. D., and R. Asselin, Adjustment of the wind field to geopotential data in a primitive equations model, J. Atmos. Sci., 29, 1059-1063, 1972.

Schmidt, H., NOAA's long-term goals, Preprint Volume, Fifth Symposium on Meteorological Observations and Instrumentation, April 11-15, 1983,

Toronto, Ont., Can., AMS, Boston, Mass., 1983.

Shapiro, M. A., D. C. Hogg, and C. G. Little, The Wave Propagation Laboratory Profiler system and its applications, Preprint Volume, Fifth Symposium on Meteorological Observations and Instrumentation, April 11-15, 1983, Toronto, Ont., Can., AMS, Boston, Mass., 1983.

Strauch, R. G., Radar measurement of tropospheric wind profiles, Preprint Volume, 20th Conference on Radar Meteorology, Nov. 30-Dec. 3, 1981, Boston, Mass., AMS, Boston, Mass., 1981.

Strauch, R. G., and A. Cohen, Atmospheric remote sensing with laser radar, in Remote Sensing of the Troposphere, V. E. Derr (ed.), U. S. Government Printing Office, Washington, DC, 1972.

Strauch, R. G., M. T. Decker, and D. C. Hogg, An automatic profiler of the troposphere, Preprint Volume, 20th Aerospace Sciences Meeting, Jan. 11-14, 1982, Orlando, Florida, AIAA, New York, N. Y., 1982.

UCAR, The National STORM Program: Framework for a Plan, University Corporation for Atmospheric Research, Boulder, Colorado, 1982.

Williamson, D. L., and R. E. Dickinson, Periodic updating of meteorological variables, J. Atmos. Sci., 29, 190-193, 1972.

Woodman, R. F., and A. Guillen, Radar observations of winds and turbulence in the stratosphere and mesosphere, J. Atmos. Sci., 31, 493-505, 1974.

Zipser, E., Nowcasting and very-short-range forecasting, in The National STORM Program: Scientific and Technological Bases and Major Objectives, R. A. Anthes (ed.), University Corporation for Atmospheric Research, Boulder, Colorado, 1983.

On Aliasing Problems in Vertical Velocity Measurement by VHF Radar

FU-SHONG KUO, JURGEN RÖTTGER, JIH-KWIN CHAO,
CHAO-HAN LIU AND MIGUEL FOLKMAR LARSEN

Reprinted from Proceedings of the National Science Council
Part A: Physical Science and Engineering
Vol. 8, No. 3, pp. 183-190, July 1984

National Science Council
Taipei, Taiwan
Republic of China

Proc. Natl. Sci. Counc. ROC(A)
Vol. 8, No. 3, 1984. pp. 183-190

On Aliasing Problems in Vertical Velocity Measurement by VHF Radar

FU-SHONG KUO*, JURGEN RÖTTGER**, JIH-KWIN CHAO***,
CHAO-HAN LIU**** AND MIGUEL FOLKMAR LARSEN*****

*Department of Physics
National Central University
Chung-Li, Taiwan
Republic of China
**EISCAT Scientific Association
Box 705 S-981 27 Kiruna
Sweden
***Department of Atmospheric Physics
National Central University
Chung-Li, Taiwan
Republic of China
****Department of Electrical Engineering
University of Illinois
Urbana, Illinois 61801
U.S.A.
*****School of Electrical Engineering
Cornell University
Ithaca, NY 14853
U.S.A.

(Received, 28 February 1984; Accepted, 18 May 1984)

ABSTRACT

Partial and total aliasing problems in spectral analysis of the vertical velocity measurement by single VHF radar beam are analyzed, and an iteration technique for the aliasing correction is presented. Also, a systematic criterion for the total aliasing correction of vertical velocity measurement by three spatially separated VHF radar beams is presented and discussed.

Key words: VHF radar technique, aliasing probrem and its correction

Introduction

Spectral analysis and autocorrelation analysis are two major techniques which are used in measuring the vertical velocity by radar. The velocity v of the scattering target in atmosphere along the radar beam direction is linearly related to the Doppler frequency f by $v = \frac{\lambda}{2} f$, where λ is the radar wavelength. The mean velocity $\bar{v}$ of the atmosphere layer within a certain time period is naturally related to the mean frequency of the Doppler spectrum of the radar echo signals by $\bar{v} = \frac{\lambda}{2} \bar{f}$. The mean frequencies were obtained either directly from the Doppler spectrum which was the finite Fourier transform of the radar echo signals, or from the phase angle of the complex autocorrelation function at the first time-lag, while the aliasing problems have not been paid enough attention to. Careful study of the periodic nature of Doppler spectrum led us to conclude that the aliasing problems are serious enough to cause grave data error which is harmful to the phenomena under investigation. In principle, the aliasing can be corrected using a procedure developed by Sato and Woodman [1], however, an alternative procedure is presented in this paper.

Aliasing in Spectral Analysis and its Correction

There exist two types of aliasing in the Doppler spectrum, one is the nonuniform amplification introduced by the preintegration of radar echo signals during data acquisition process, the other one is the aliasing of the frequencies of the spectrum resulted from the periodic nature of finite Fourier transform.

The nonuniform amplification problem can be understood as follows. The output complex data $Z(t_k)$ at time t_k after on-line preintegration of n consecutive signals of a plane wave of frequency f, $e^{i2\pi ft}$, is given by,

$$Z(t_k) = \frac{1}{n}\sum_{\ell=0}^{n-1} \exp\left[i2\pi f\left(t_{k-1} + \ell\frac{\Delta t}{n}\right)\right]$$

$$= g(f)\exp\left[i2\pi f t_{k-1}\right]. \qquad (1)$$

where

$$g(f) = \begin{cases} 1 & \text{for } f = 0 \\ \frac{1}{n}\dfrac{1-\exp(i2\pi f\Delta t)}{1-\exp(i2\pi f\Delta t/n)} & \text{for } f \neq 0. \end{cases} \qquad (2)$$

So the power of the original plane wave with frequency f is amplified by a preintegration-amplification factor $H(f)$ given by

$$H(f) = |g(f)|^2 = \frac{1}{n^2}\frac{1-\cos(2\pi f\Delta t)}{1-\cos(2\pi f\Delta t/n)}. \qquad (3)$$

The number of radar echo signals n and time interval Δt of preintegration are preset by the experiment. In our example data which will be described later in this section, $n = 256$ and $\Delta t = 1.03$ seconds, the dependence of $H(f)$ on the Doppler frequency f as shown in Fig. 1, clearly shows that the non-uniformity of the preintegration-amplification factor is significant.

Conventionally, the so-called non-uniform amplification problem is really associated with the fact that any filtering done on the data will affect the data and to restore the original property of the data the transfer function of the filter should be used. Coherent integration amounts to a low-pass filter, and Fig. 1 is indeed the magnitude of the transfer function of that filter. In practice, the coherent integration time had better be chosen such that it will not gravely affect the Doppler spectrum.

The aliasing of some frequencies of the Doppler spectrum can be explained by the following analysis of the periodic nature of finite Fourier transformation,

$$Z(t_k) = \frac{1}{\sqrt{N}}\sum_{n=0}^{N-1} \tilde{Z}(f_n)\, e^{-i2\pi nk/N}$$

$$\tilde{Z}(f_n) = \frac{1}{\sqrt{N}}\sum_{k=0}^{N-1} Z(t_k)\, e^{+i2\pi nk/N} \qquad (4)$$

where,

$$t_k = K\Delta t$$

$$f_n = n\Delta f = \frac{n}{N\Delta t}$$

$$k, n, = 0, 1, 2, \ldots, N-1.$$

It can be easily seen from Eq. (4) that,

$$\tilde{Z}(f_n + N\Delta f) = \tilde{Z}(f_n)$$

and so is the Doppler spectrum,

$$D(f_n + N\Delta f) = D(f_n) \qquad (5)$$

because the Doppler spectrum is given by

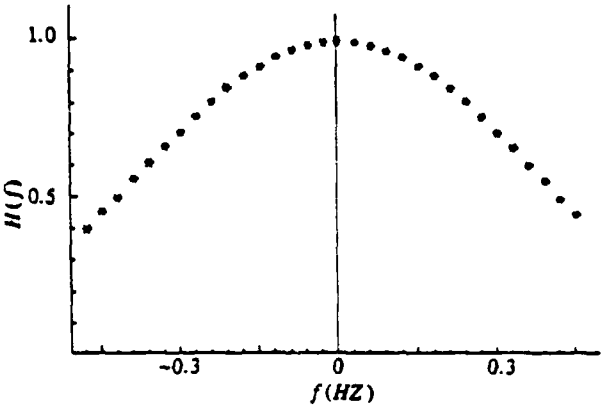

Fig. 1. Preintegrate amplification factor $H(f)$ at different frequencies.

$$D(f_n) = |\tilde{Z}(f_n)|^2.$$

The power spectrum of the radar echo scattered from the clear atmosphere turbulence tends to be Gaussian which is symmetric with respect to its mean $\bar{f}$ as expressed in Fig. 2a. However, the finite Fourier transform always presents the spectrum in the frequency domain between $-\frac{N}{2}\Delta f$ and $(\frac{N}{2} - 1)\Delta f$ with its center at zero frequency, and that results in the aliasing of some frequencies by either $N\Delta f$ or $-N\Delta f$ due to the periodic nature of Doppler spectrum as expressed by Eq. (5). This kind of aliased spectrum is demonstrated in Fig. 2b. For the convenience of further discussion, let's call this type of aliasing as partial aliasing of the Doppler spectrum.

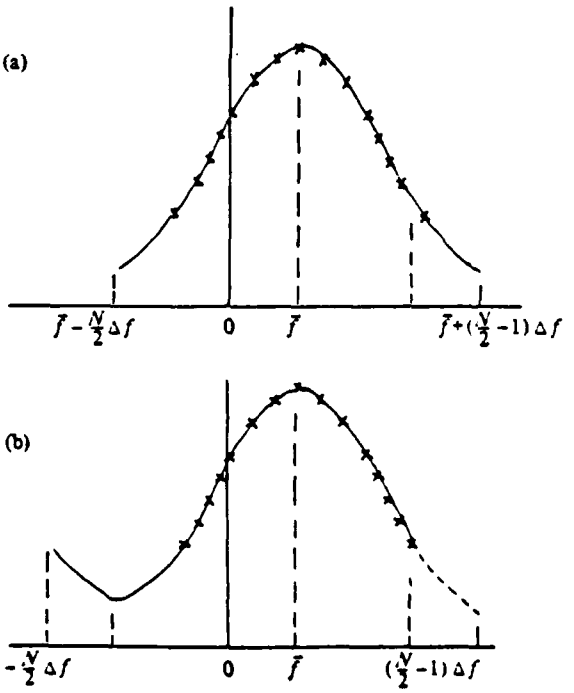

Fig. 2. (a) Original power spectrum.
(b) Partially aliased power spectrum of (a).

Practically, the partial aliasing of the Doppler spectrum as shown in Fig. 2b can be reconstructed to its real form as shown in Fig. 2a by an iteration technique. The iteration process is as follows, first, calculate the mean frequency $\bar{f}$ of the power spectrum obtained directly from finite Fourier transform, then shift the frequency domain of the spectrum from $[-\frac{N}{2}\Delta f, (\frac{N}{2}-1)\Delta f]$ to $[\bar{f}-\frac{N}{2}\Delta f, \bar{f}+(\frac{N}{2}-1)\Delta f]$ by applying Eq. (5), followed by recalculating $\bar{f}$ and shifting the spectrum domain by putting the center of the spectrum at the newly obtained mean frequency. Repeat this process again and again until the mean frequency $\bar{f}$ converges to $\bar{f}^*$.

The following examples are from the result of our analysis of the sample of SOUSY data, which were taken with SOUSY-VHF radar by Max-Planck-Institute für Aeronomie. The radar is located in the Harz Mountain in Northern Germany. Pulse modulation, choerent detection and on-line pre-integration were applied, and the data were stored on magnetic tape for off-line evaluation. The radar operated at a frequency of 53 MHz and the beam was pointed upward vertically. 256 consecutive radar echo signals were on-line preintegrated with a time interval of 1.03 seconds to give one record, each record includes 105 complex data for 105 different height ranges between 0.9 km and 16.65 km, with height resolution 0.15 km. There are 21444 records in our sample tape.

To obtain the mean vertical velocity of each height range within certain time period by spectral analysis technique, 32 consecutive complex data with a time period of 32.96 seconds (=32x1.03) for each height range were analyzed by FFT to obtain a power spectrum. Then, 8 consecutive power spectra were averaged to give a smoother Doppler spectrum, 82 such Doppler spectra were obtained for each height range, and each Doppler spectrum covers a time interval of 4.39 minutes (=32.96x8 seconds). There were a total number of 8610 (=82x105) Doppler spectra, among them 4 sample spectra are demonstrated in Figs. 3 (a,b,c,d), where partial aliasing can be clearly seen.

The mean frequency $\bar{f}$ of each Doppler spectrum is calculated by the equation,

$$\bar{f} = \sum_k D_k f_k / \sum_k D_k \qquad (6)$$

where D_k is the power of the spectrum at frequency f_k. The partial aliasing of each of all the 8610 Doppler spectra was corrected by the iteration technique until $\bar{f}$ converges to $\bar{f}^*$. The corresponding spectra in Figs. 3 (a,b,c,d) after aliasing correction were replotted in Figs. 3 (a',b',c',d'), where each spectrum looks much more symmetric and much closer to Gaussian distribution which was represented by the smooth curve in the same figure. The comparisons between the mean velocity $\bar{v}$ converted from the mean frequency $\bar{f}$ of each spectrum in Figs. 3 (a,b,c,d) and the mean velocity $\bar{v}^*$ obtained from the corresponding

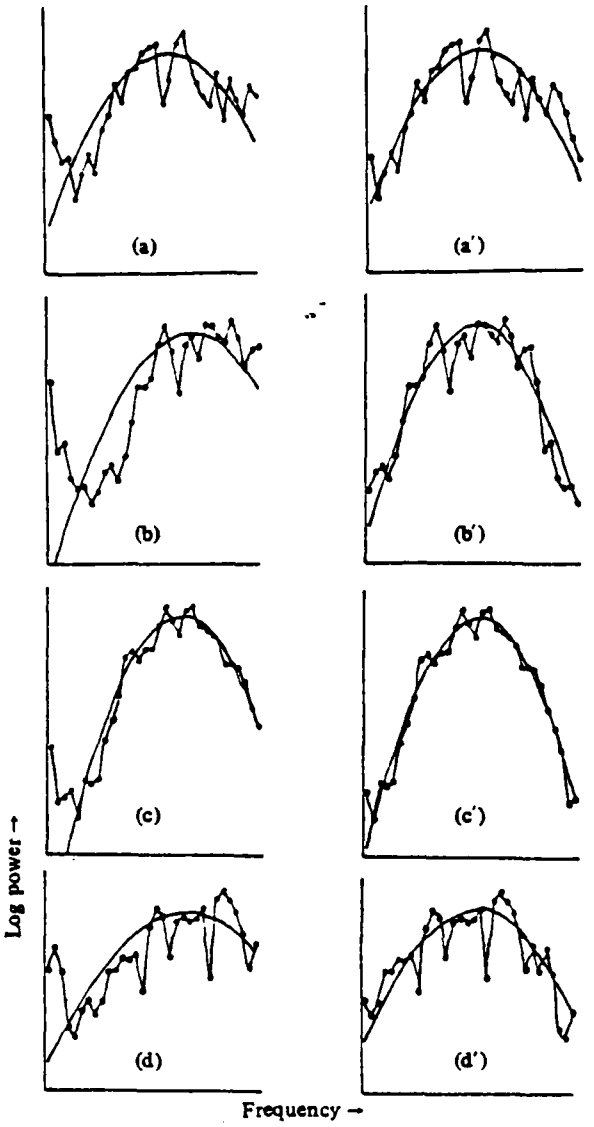

Fig. 3. (a,b,c,d) Examples of power spectra obtained by finite-Fourier transforms. Partial aliasings are clearly seen.
(a',b',c',d',) Corresponding power spectra of fig. 3(a,b,c,d) after aliasing correction by iteration technique.

spectrum in Figs. 3 (a',b',c',d') are presented in Table 1, which shows that partial aliasing of Doppler spectrum may cause the velocity measurement error as high as 80%.

Partial aliasing is due to the aliasing of only part of the frequencies. On the other hand, there may also exist

Table 1. Comparison of Vertical Velocity v Before Aliasing Correction and $\bar{v}^*$ After Aliasing Correction

Sample	v (cm/sec)	$\bar{v}^*$ (cm/sec)	error (%)
a	15.4	27.5	79
b	45.2	62.4	38
c	30.3	31.6	4.3
d	40.2	57.3	43

the possibility that all the frequencies of the spectrum are aliased by the same number of cycles, namely, by $nN\Delta f$ where n is an integer. Also, for convenience of discussion, let's call this type of aliasing as total aliasing of Doppler spectrum. It is clear that in the case of total aliasing, the mean frequency $\bar{f}^*$ should be corrected by $nN\Delta f$. In principle, the vertical velocity can be any one of the following values,

$$\frac{\lambda}{2}(f^* + nN\Delta f),\ n = 0, \pm 1, \pm 2, \ldots$$

Experience from conventional measurements suggests that the vertical velocity is usually in the order smaller than 1 m/sec, and that will limit n to be either 0 or ±1. We still have to tell which one of 0, +1, and -1 for n is closest to reality. For single radar beam measurement, the possible solution comes from the comparison between the present velocity V_p^*, and both the velocity one time step before, V_b^* and the velocity one time step after, V_a^*. If both $V_p^* - V_a^*$ and $V_p^* - V_b^*$ are larger than $\frac{\lambda}{2}(\frac{N}{2}\Delta f)$, then $V_p^* - \frac{\lambda}{2}N\Delta f$ is probably closer to reality than V_p^*. On the contrary, if both $V_p^* - V_a^*$ and $V_p^* - V_b^*$ are smaller than $-\frac{\lambda}{2}(\frac{N}{2}\Delta f)$, then $V_p^* + \frac{\lambda}{2}N\Delta f$ is probably better than V_p^*. Otherwise, V_p^* is probably the best choice. Or, we may also compare the present velocity with that of the nearest upper and the nearest lower height ranges and do the same type of correction.

For three or more spatially separated VHF radar beam measurement, still another type of correction of total aliasing is possible. The following section is an example.

Total Aliasing Correction of Vertical Velocities Measured by Three Spatially Separated VHF Radar Beams

The data evaluated in this section were taken with the same radar by the same institute as described in the previous section, starting from 4PM, October 28, 1981 and lasting for 16 days. The radar was operated either continuously for 12 minutes then stopped for the remaining 48 minutes of each hour, or continuously operating for many hours, there are a total number of 485 time intervals of operation with 12 minutes for each, and the data covers 1.35 km-19 km height range. Three antenna sets are arranged as shown in Fig. 4, with each set operating in cyclic order for 1/3 seconds then stopping for 2/3 seconds alternatively.

The raw data were processed by Max-Planck-Institute for each height range to obtain the two moments of the power spectrum of radar echo signals from each radar beam of each 12 minutes time period by the autocorrelation method.

The autocorrelation function of a coherently detected radar echo signal $E(t)$ is,

$$C(\tau) = \langle E(t)E^*(t+\tau)\rangle$$

the power spectrum of the signal is,

$$D(\omega) = \frac{1}{2\pi}\int C(\tau)\exp(-i\omega\tau)d\tau$$

here, t = time, ω = angular frequency, τ = temporal displacement and * denotes the complex conjugates. The first three moments m_0, m_1, m_2 of the spectrum yield essential parameters of the radar echo, namely, the power P, the mean frequency $\bar{f}$ and the spectral width σ. These are,

$$P = m_0 = \int D(\omega)d\omega$$

$$\bar{f} = \frac{m_1}{m_2} \text{ with } m_1 = \int \omega D(\omega)d\omega$$

$$\sigma = \sqrt{\frac{m_2}{m_0} - \left(\frac{m_1}{m_0}\right)^2} \text{ with } m_2 = \int \omega^2 D(\omega)d\omega.$$

The three moments can also be deduced directly from the autocorrelation function (Woodman and Guillen [2]) yielding

$$P = C(\tau_0) \qquad (\tau_0 = 0)$$

$$\bar{f} = \frac{\psi(\tau_1)}{\tau_1} \qquad (\tau_1 = \text{first time lag})$$

$$\sigma = \left[\frac{2\{1 - A(\tau_1)/A(\tau_0)\}}{\tau_1^2}\right]^{1/2} \tag{7}$$

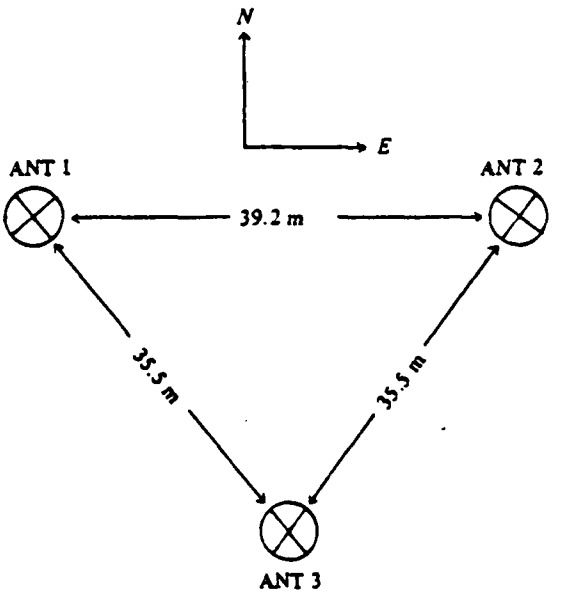

Fig. 4. Arrangement of 3 spatially separated antenna subsystems, where ⊗ denotes the center of antenna subsystem, each containing 32 yagis, and the average transmitter power was ≈ 20 kw.

where $A(\tau)$ is the amplitude and $\psi(\tau)$ is the phase of the autocorrelation function,

$$C(\tau) = A(\tau) \exp\,[i\psi(\tau)]$$

or

$$\psi(\tau) = \tan^{-1} \frac{I_m C(\tau)}{R_e C(\tau)}. \tag{8}$$

Since the arctangent function is a periodic function with period 2π, and its principal value is defined in the range between $+\pi$ and $-\pi$, so the phase ψ given by Eq. (8) can be aliased from its true value by $2n\pi$, $n = 1, 2, \ldots$. This is just the case of total aliasing, its possible solution can be observed through comparisons among the three phases ψ_1, ψ_2, ψ_3 of the three autocorrelation functions of the three respective radar echo signals. Since the separation between any two of the three antenna sets is less than 40 meters, which is small compared with the scale of the atmospheric motion on the 12 minutes average, it is natural to expect that the distributions of $\psi_i - \psi_j$ $(i,j = 1,2,3)$ should follow Gaussian distribution with zero mean. That means that a smaller absolute value of $\psi_i - \psi_j$ is always more probable than a larger absolute value of $\psi_i - \psi_j$. This principle highlights the possibility of correcting the total aliasing, and the following four cases as demonstrated in Fig. 5 (a,b,c,d) can be corrected as follows:

Case 1. In Fig. 5a

$|\psi_i - \psi_k| > \pi$, $|\psi_j - \psi_k| > \pi$ and $-\pi < \psi_k < -\frac{\pi}{2}$. Correct ψ_k by $+2\pi$, i.e., $\tilde{\psi}_k = \psi_k + 2\pi$, then both $|\psi_i - \tilde{\psi}_k|$ become less than π. We can see that $\tilde{\psi}_k$ is probably closer to reality than ψ_k.

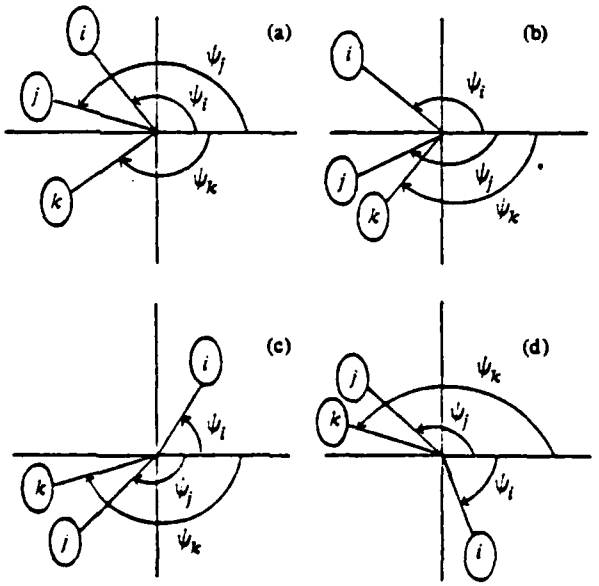

Fig. 5. Separations of three phases ψ_i, ψ_j, ψ_k (i,j,k denote 1,2,3) of the three autocorrelation functions of three radar echo singnals.

Case 2. In Fig. 5b

With similar reason of Case 1, we may correct ψ_i to $\tilde{\psi}_i$ by $\tilde{\psi}_i = \psi_i - 2\pi$.

Case 3. In Fig. 5c

$|\psi_i - \psi_j| > \pi$, $|\psi_i - \psi_k| > \pi$ and $0 < \psi_i < \frac{\pi}{2}$. In principle we may correct ψ_i to $\tilde{\psi}_i$ by $\tilde{\psi}_i = \psi_i - 2\pi$ to make both $|\psi_i - \psi_k|$ and $|\tilde{\psi}_i - \psi_j|$ less than π. However, because $|\psi_i| < \frac{\pi}{2}$ and $|\tilde{\psi}_i| > \frac{\pi}{2}$. $|\tilde{\psi}_i|$ seems to be much less probable than ψ_i to be true. So instead of correcting ψ_i, it may be better to correct ψ_j and ψ_k by $\tilde{\psi}_j = \psi_j + 2\pi$ and $\tilde{\psi}_k = \psi_k + 2\pi$.

Case 4. In Fig. 5d

With same reason of Case 3, we may correct ψ_j and ψ_k by $\tilde{\psi}_j = \psi_j - 2\pi$ and $\tilde{\psi}_k = \psi_k - 2\pi$.

As examples, the means and variances of the distributions of the phase differences, $\psi_1 - \psi_2$, $\psi_1 - \psi_3$ and $\psi_2 - \psi_3$ of each height range were calculated both before and after aliasing correction and the results were presented in Figs. 6 – 11. Figs. 6 – 8 show that the amplitude of the means $\psi_1 - \psi_2$ and $\psi_1 - \psi_3$ tend to be too large for many height ranges before aliasing corrections, while the amplitude of the means of $\psi_1 - \psi_2$, $\psi_1 - \psi_3$, and $\psi_2 - \psi_3$ are generally much closer to zero after aliasing correction, and, Figs. 6 – 11 show criteria for total aliasing correction do make sense. Also, Figs. 9 – 11 show that the variances of $\psi_i - \psi_j$ $(i,j = 1,2,3)$ become much smaller after aliasing correction, so finer distributions for $\psi_i - \psi_j$ were obtained.

It is important to make one point clear; there is no way in the autocorrelation analysis to detect the partial aliasing, much less to correct it.

Summary and Discussions

Theoretically, the mean frequency $\bar{f}$ of a power spectrum as defined by Eq. (6) and that deduced directly

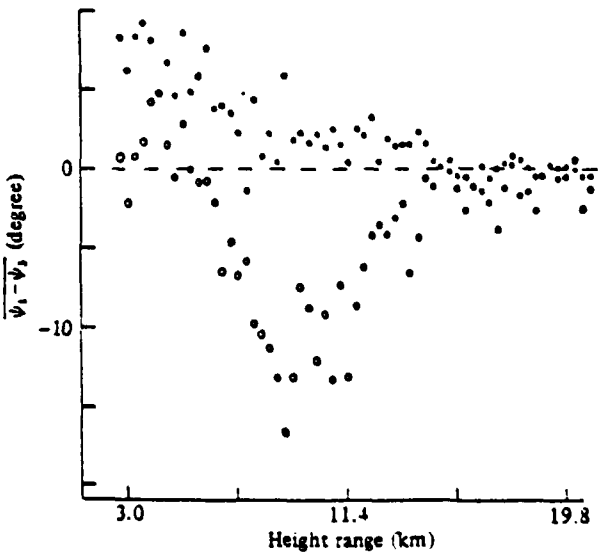

Fig. 6. $\overline{\psi_1 - \psi_2}$ at each height range before aliasing correction (○) and after aliasing correction (●).

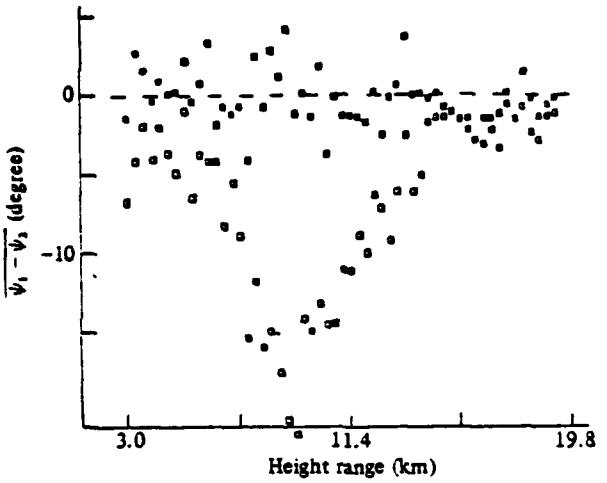

Fig. 7. $\overline{\psi_1 - \psi_2}$ at each height range before aliasing correction (□) and after aliasing correction (■).

from the autocorrelation function as given by Eq. (7) tend to be equal to each other as the time step Δt of the time series approaching to zero, and the total time interval T approaching to infinity. However, both Δt and T are finite in any practical case, and that results in the existence of partial aliasing as well as total aliasing of frequencies of the spectrum. By spectral analysis method as described in §2, both can be systematically corrected with confidence. On the contrary, there is no way by autocorrelation method to detect the partial aliasing, much less to correct it. Furthermore, the nonuniform-amplification of the spectrum, which is resulted from the on-line preintegration of radar echo signals, can be fixed by the spectral analysis but not by the autocorrelation method. That underlines the shortcoming of the autocorrelation method proposed by Woodman and Guillen [2].

The iteration method to correct the partial aliasing problem as described in §2 is very powerful to eliminate

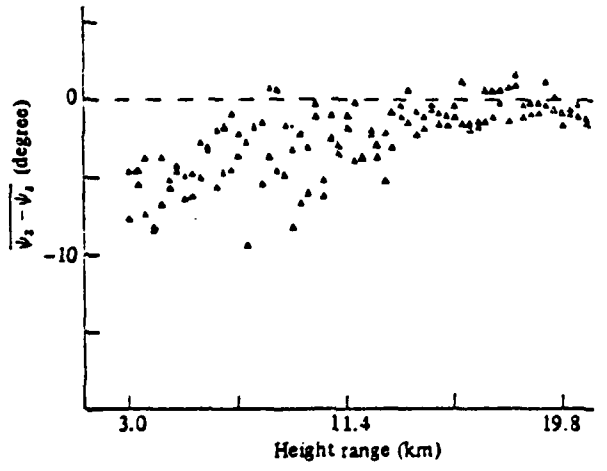

Fig. 8. $\overline{\psi_2 - \psi_3}$ at each height range before aliasing correction (△) and after aliasing correction (▲).

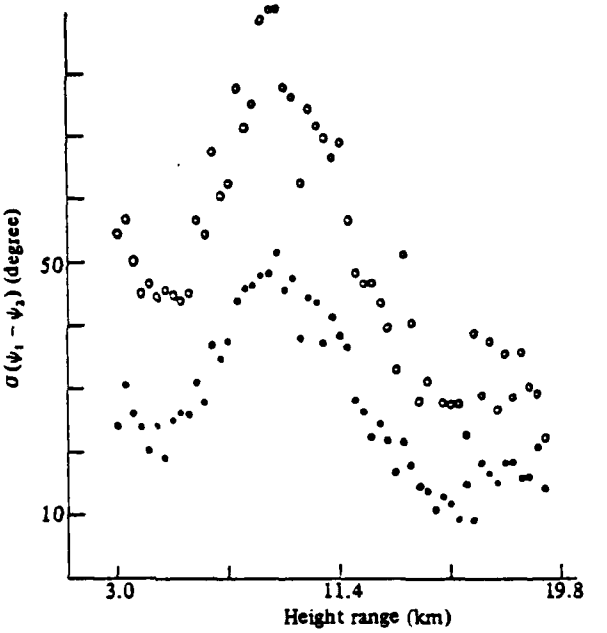

Fig. 9. Standard deviation σ of $\psi_1 - \psi_2$ distribution at each height range before aliasing correction (○) and after aliasing correction (●).

first order aliasing of spectra. However, one should be careful that it might not be applicable for second and higher order aliasing.

The total aliasing correction of vertical velocity measured by three spatially separated VHF radar echoes was based on our belief that a smaller absolute value of

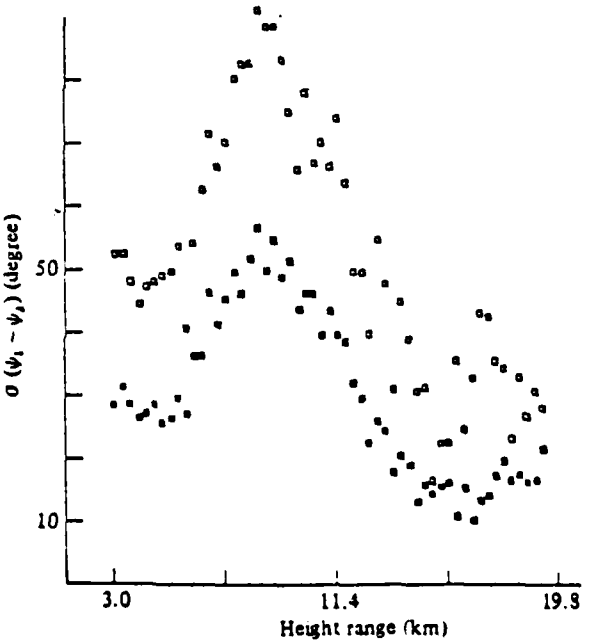

Fig. 10. Standard deviation σ of $\psi_1 - \psi_3$ distribution at each height range before aliasing correction (□) and after aliasing correction (■).

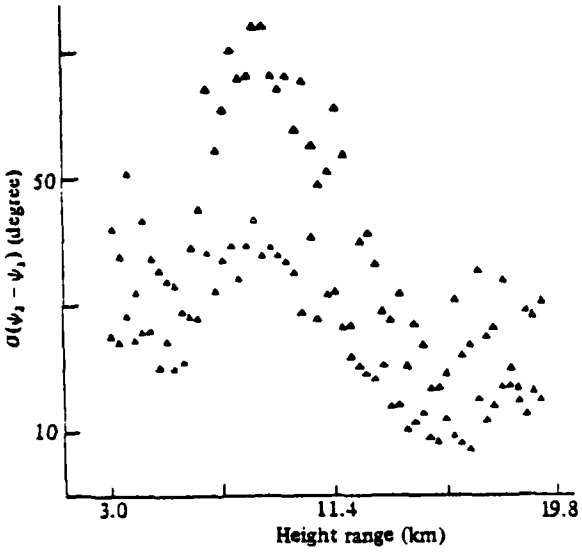

Fig. 11. Standard deviation σ of $\psi_2 - \psi_3$ distribution at each height range before aliasing correction (△) and after aliasing correction (▲).

$\psi_i - \psi_j$ is always more probable than a larger value, and we think that this also holds for samples which may be aliased because of undersampling a time series varying because of a mean vertical velocity of the reflector. Assume an atmospheric "reflector", which has an extension larger than the overlapping Fresnel zones, or antenna beams, of the 3 antennas. The reflector shall not change its shape, but shall move with constant vertical speed. We then get the 3 autocorrelation functions at the 3 antennas equal in phase and amplitude. The correlation time, i.e., the time it takes for the amplitude to change, is very long and also the correlation distance is very large, i.e., the signals at all 3 antennas are similar. Regardless of the time when the samples are taken, $\psi_i - \psi_j = 0$. This is also the case for any vertical velocity, which even may lead to higher order aliasing.

Now assume that the reflector changes its shape (say in some random manner), which results in shorter correlation time and smaller correlation distance. As a result, the phases at lags larger than the correlation time are changing randomly. Also the phases may change randomly at the 3 antennas, even at $\tau = 0$, because the spatial correlation may be lost. For lags shorter than the correlation time, the phases are distributed (say Gaussian) around a mean phase, which is given by the mean vertical velocity. Assuming that the mean vertical velocity is similar overhead all 3 antennas, the mean phases must be similar. The differences $\psi_i - \psi_j$ are distributed around zero. The width of the distribution of $\psi_i - \psi_j$ does not depend on the mean vertical velocity rather on the random (turbulent) velocity fluctuations. Thus, the wider this distribution, the more variable is the probed atmospheric region. This variability is due to the turbulent fluctuations of the region of the "reflector" itself, as well as due to the fact that this reflector is moving horizontally.

Then we propose the following criterion to treat the data. Firstly, we assume that aliasing due to mean vertical velocity is unlikely (Nyquist vertical velocity is 2.7 m/sec), but it may occur due to fluctuations. There then is a choice to select among good data which will not be corrected, marginal data which can be corrected, and bad data which have to be corrected. For example, it can be fair that only those sets of data with $|\psi_i - \psi_j|$ larger than a specified variance σ (say, 3σ of a Gaussian distribution) are to be corrected and this variance σ should be predetermined by the data of a rather quiet time period. Of course, Only those data sets which indicate a sufficient signal-to-noise ratio shall be considered. Still, this correction does not eliminate any aliasing which may be due to a large vertical velocity (mean), which can be checked only when comparing ψ_1, ψ_2, ψ_3 with another ψ measured with a higher sampling rate.

Additionally, any sets of $\psi_i - \psi_j$ which do not belong to a Gaussian distribution, e.g., rectangular distribution in case of strong fluctuations, should be taken with great care. Instead of correcting, a more acceptable approach from our point of view would discard those data and not using them to estimate the mean vertical velocity, but still use the criterion to determine times and ranges which were strongly variable (i.e. most likely turbulent).

Acknowledgements

One of the authors (F.S. Kuo) wants to thank EISCAT and Cornell University for their hospitality, where part of this work is carried out, and to thank National Science Council for the generous support of his traveling cost.

References

1. Sato, T. and R.F. Woodman. 1982. Spectral parameter estimation of CAT radar echoes in the presence of fading clutter. *Radio Science*, 17, =2, 817-826.
2. Woodman, R.F. and A. Guillen. 1974. Radar observations of winds and trubulence in the stratosphere and mesosphere. *J. Atmos. Sci.*, 31, 493-505.

以極高頻雷達波束測量垂直運動速度的頻率錯位問題

郭富雄* • J. Röttger** • 趙寄昆*** • 劉兆漢**** • M.F. Larsen*****

* 國立中央大學物理系
** EISCAT Scientific Association
*** 國立中央大學大氣物理研究所
**** 伊利諾大學電機系
***** 康乃爾大學電機系

摘　要

以極高頻雷達垂直波束測量大氣垂直運動速度，其回射信號之都卜勒波譜的平均頻率直接決定運動速度，但在作波譜分析時，吾人立即遭遇最重的頻率錯位問題，錯位問題分成部份的及全面的，本文對此問題作了詳盡的分析並提出系統化的解決辦法，同時，對於以三個分隔的垂直波束測量速度時所面臨的另一問題，亦作了分析及討論。

Reprinted from MONTHLY WEATHER REVIEW, Vol. 111, No. 10, October 1983
American Meteorological Society
Printed in U. S. A.

Can a VHF Doppler Radar Provide Synoptic Wind Data? A Comparison of 30 Days of Radar and Radiosonde Data

MIGUEL FOLKMAR LARSEN

School of Electrical Engineering, Cornell University, Ithaca, NY 14853

(Manuscript received 4 January 1983, in final form 16 June 1983)

ABSTRACT

A number of experiments have shown that UHF and VHF Doppler radars can make "clear air" wind measurements in the troposphere and lower stratosphere, even in the presence of clouds and precipitation. Past comparisons of radar and rawinsonde profiles for a single day have shown good agreement between the two within the limitations imposed by the spatial separation between the two measurements. However, the accuracy of the measurement does not insure that the data are synoptically significant. A comparison of 30 days of radiosonde geopotential height and wind data and radar data from Alaska was carried out to determine the applicability of the radar data to synoptic meteorology.

Rawinsonde and radar wind time series at six heights between 3.79 and 14.79 km altitude were compared and the rms differences calculated. The two independent wind measurements were also compared to the geostrophic wind obtained from the geopotential height fields generated by applying the Cressman objective analysis scheme to data from five radiosonde stations surrounding the radar site. The two independent wind measurements were most similar with a difference of 3–4 m s^{-1}. The radar and balloon winds both differed from the geostrophic winds by 5–6 m s^{-1}. The rms differences decreased when the radar winds were averaged over longer time intervals. The cross correlation between the measured and geostrophic winds was found to be ~0.75 and essentially independent of height over the altitude range studied.

1. Introduction

The number of sensitive VHF and UHF Doppler radars being used for atmospheric research has increased considerably since Woodman and Guillen (1974) first reported on their measurements. Radars operating at wavelengths from tens of centimeters to several meters measure the winds from the Doppler shift of the signal backscattered from turbulent variations in the refractive index. Typical height and time resolutions are of the order of hundreds of meters and several minutes. The technique and some of the early results have been reviewed by Gage and Balsley (1978), Röttger (1980) and Harper and Gordon (1980).

The first research applications of the long-wavelength radars were in the area of microscale dynamics, including turbulence in the troposphere and lower stratosphere and wave dynamics at scale sizes typical of gravity waves. Over the past few years there has been increasing interest in using the radar measurements for synoptic research and as part of the standard observational network. Larsen and Röttger (1982) have reviewed research applications, and Balsley and Gage (1982) have discussed some of the considerations involved in establishing an operational observing system. Carlson and Sundararaman (1982) have made strong arguments for the economic feasibility of implementing such a network. One of the most ambitious operational projects utilizing the radar technique is part of the PROFS (Prototype Regional Observing and Forecasting System) program designed to improve mesoscale forecasting over periods of a day or less. PROFS includes a network of three VHF radars located in a triangle centered at Boulder, Colorado. Radar wind profiles are routinely processed and transmitted to the forecasting office once an hour to aid in short-range forecasting (Hogg *et al.*, 1980; Strauch, 1981; Strauch *et al.*, 1982).

The relatively low cost of establishing a facility is part of the appeal of the radar systems. Also, very little maintenance or other manual intervention is required once the facility is in operation (see, e.g., Balsley *et al.*, 1980). The present study was undertaken to determine if a VHF radar system of the type that would most likely be used operationally can provide wind data that is synoptically meaningful. The radar provides a very accurate wind measurement, i.e., a very accurate measurement of the velocity of the turbulent scatterers in the direction parallel to the beam. The attainable accuracy is much greater than what would be useful in practice. However, the measurement may be contaminated with high-frequency subsynoptic-scale noise, making the data unusable. Also, the VHF radars typically operate with large fixed dipole arrays that look within a few degrees of vertical. Thus scans of large horizontal areas to determine the wind representative of some area greater than a predetermined horizontal scale size are not possible. However, it may be that

averaging high time-resolution wind profiles can provide a suitable filtering. The next sections will investigate the amount of averaging that is necessary.

A comparison limited to the rawinsonde and radar winds would not reveal if the differences are due to the peculiarities of one measurement system or the other. Therefore, the two independent wind measurements were also compared to the geostrophic wind calculated from a grid of geopotential heights derived from nearby radiosonde measurements. The geostrophic wind then provides an independent standard for comparison.

2. Synoptic representativeness

The general meaning of synoptic representativeness is clear, based on the discussion above, but a specific quantitative comparison was needed for this study. The problem is, in fact, closely related to the problems of data assimilation and objective analysis for numerical models (see e.g., Bengtsson *et al.*, 1981). The latter attempts to treat a set of observations in such a way that high-frequency waves that lead to numerical instabilities are eliminated. A balance condition of one kind or another is used to accomplish this, the simplest being a geostrophic balance (e.g., Cressman, 1959) and the most involved being the balance derived from the model dynamics and termed normal mode initialization (e.g., Daley, 1981).

In this study I will compare radar wind data taken over a 30-day period from 1 March to 1 April 1979 and radiosonde data taken at the standard observational hours during the same period. The radar is located at Poker Flat, Alaska [see Balsley *et al.* (1980) for a description], and the nearest radiosonde station is at Fairbanks, 35 km southeast of the radar. The radar measures one complete wind profile every 4 min between the surface and 14.79 km, but these high time-resolution measurements are likely to be contaminated by high-frequency meteorological "noise." In order to test whether or not the radar can provide useful synoptic-scale wind information, comparisons were made between the geostrophic wind derived by applying an objective analysis scheme to the geopotential height data from five surrounding radiosonde stations and the radar winds averaged over various time intervals.

A test of geostrophy may not be the best test of synoptic representativeness, but a simple, yet useful, comparison was needed for the purpose of this initial study. Also, the differences between the radar, rawinsonde and geostrophic winds are of interest from the point of view of the multivariate objective analysis schemes that use geostrophy to relate height–height autocorrelations to the height–wind cross correlations (e.g., Rutherford, 1972; Schlatter, 1975; Schlatter *et al.*, 1976; Bergman, 1979; Bengtsson *et al.*, 1981; Lorenc, 1981). Generally, the wind measurements are used to provide information on the geopotential height gradients and these are used to formulate the initial state for a model integration. The results of this study show that the radar and rawinsonde measurements are most similar in the rms (root-mean-square) sense, and either wind measurement differs from the geostrophic wind by a larger amount than the difference between the two wind measurements.

I will describe the radar and radiosonde data sets in the next section. Radar and rawinsonde wind measurements are compared in the following section. Next, radar and rawinsonde measurements are compared to the geostrophic winds derived from the geopotential height data. The last section contains a general discussion of the implications of the results.

3. Description of the data sets

During the spring of 1979, the Poker Flat MST radar operated with a 100 m × 100 m fixed dipole array. The antenna size has since been expanded to 200 m × 200 m. The horizontal wind vector was measured using two beams pointed 15° off vertical, one with an azimuth pointing close to north and one pointing close to east. Corrections were applied to the data to get the exact zonal and meridional wind components. One complete wind profile was obtained every 4 min with a height resolution of 2.2 km. In the troposphere and lower stratosphere wind data were routinely available at six consecutive heights beginning at 3.79 km altitude. All altitudes for radar data referred to from here on are at the center of the range gate. The wind measurement is, in some sense, an average over a 2.2 km height range weighted by the intensity of the turbulent layers in the volume illuminated by the radar beam, and, as Sato and Fukao (1982) have pointed out, having a number of turbulent layers withn the range gate can lead to errors in the measurement if there is a strong shear across the range gate. However, such an effect will not be considered further here.

The signal voltages measured by the receiver are Fourier transformed to obtain the Doppler spectrum. The frequency spectrum measured by scattering from a turbulent process will be Gaussian for a normal random process as discussed by Woodman and Guillen (1974) and others. The accuracy with which the velocity of the turbulent scatterers in the radar volume can be determined is then limited only by the rate at which the signal is sampled and the accuracy with which the Gaussian can be fit to the spectrum (see e.g., Fukao *et al.*, 1982). Accuracies better than 1 cm s^{-1} can be achieved in practice, but there is usually no need to measure the horizontal wind components that accurately. The error for the radar data discussed here is ~ 1 m s^{-1}. When all three wind components are measured simultaneously, the signals from the vertical beam are coherently integrated for a longer time than the signals from the off-vertical beams to attain the much higher accuracy needed for vertical velocity measurements.

The horizontal vector winds were derived from the off-vertical wind components with the assumption that the vertical velocity was negligible. In most cases such an assumption is justified, as more recent data sets have shown when all three wind components were measured (T. Riddle, Aeronomy Laboratory, NOAA, private communication, 1982). However, there are times when the vertical velocity can make a significant contribution over a period spanning several consecutive profiles. In order to minimize any such effect, the radar wind data were averaged over an hour. The time series of the hourly-average zonal and meridional wind components are plotted in Fig. 1 taken from Larsen *et al.* (1982).

The radiosonde data provided by the National Climatic Center are from the five nearest National Weather Service (NWS) radiosonde stations as shown in Fig. 2. Only balloon launches at 0000 and 1200 GMT are available for the period discussed here. No supplemental launches are included in the data set. The radiosonde station closest to Poker Flat is at Fairbanks, 35 km southeast of the radar site. Anchorage, McGrath, Barter Island and Yakutat are 455, 476, 572 and 764 km from the radar site, respectively.

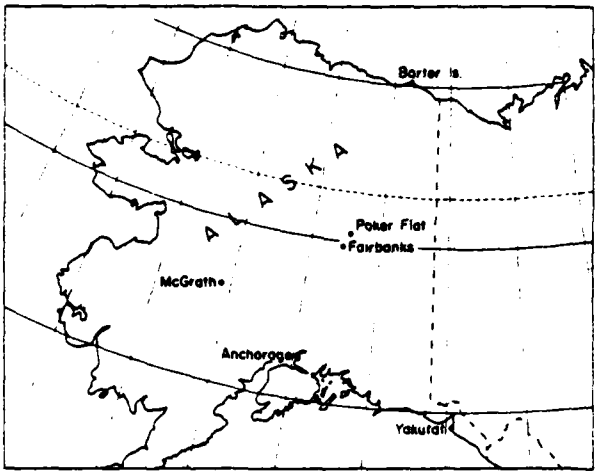

FIG. 2. Map showing the location of the five radiosonde stations closest to the site of the Poker Flat radar.

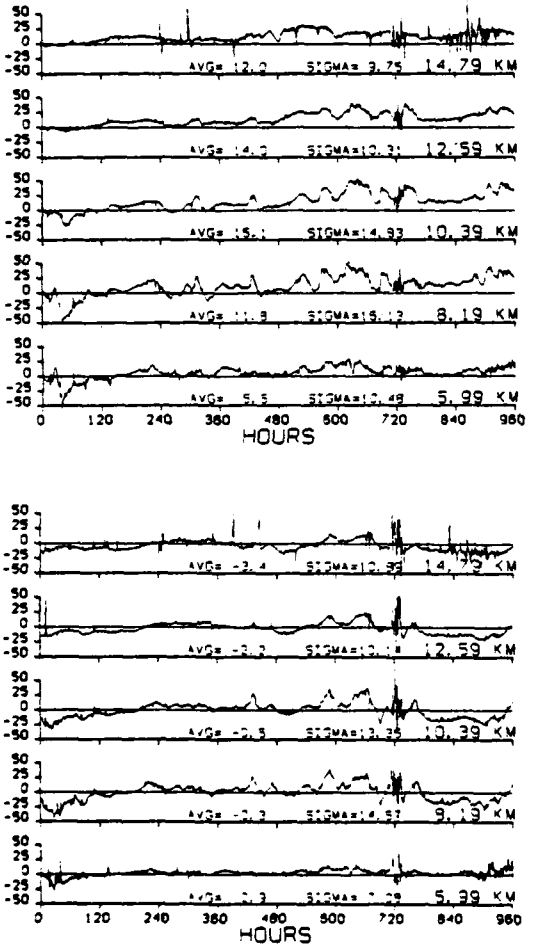

FIG. 1. Original data set of 40 days of hourly values measured by the Poker Flat, Alaska MST radar beginning on 25 February and ending on 5 April 1979. The top half of the figure is for the zonal wind and the bottom half for the meridional wind component. Only the period from 1 March to 1 April was used in the study.

The balloon wind data were interpolated linearly between the two nearest significant levels to the altitude corresponding to the center of each of the radar range gates. The interpolation was applied independently to the wind speed and the wind direction. The pressure at the seven different radar heights was determined from the Fairbanks radiosonde data. The formula for a hydrostatic atmosphere with a constant lapse rate was then used to interpolate the pressure between the two nearest significant levels, and the same formula was applied to the radiosonde data from the other four stations to find the height of the pressure surface intersecting the center of each of the radar range gates.

4. Comparison of radar and rawinsonde wind measurements

The rawinsonde and radar winds for the period from 1 March to 1 April 1979 are plotted in Fig. 3 for seven consecutive heights. The heavy solid line is the rawinsonde measurement and the light dashed line the radar measurement. The signal-to-noise ratio at 16.99 km is too low to derive a meaningful signal from the echoes, but the time series at this height have been plotted for reference, nonetheless. The radar winds are 1 h averages, as mentioned previously, while the rawinsonde data are from a single ascent. The rms difference between the two measurements is indicated by the quantity labeled SIG (sigma).

The two curves follow each other very closely until day 78 but deviate significantly from each other after that. The rms differences range from a minimum of 3.21 m s^{-1} to a maximum of 9.30 m s^{-1} in the zonal

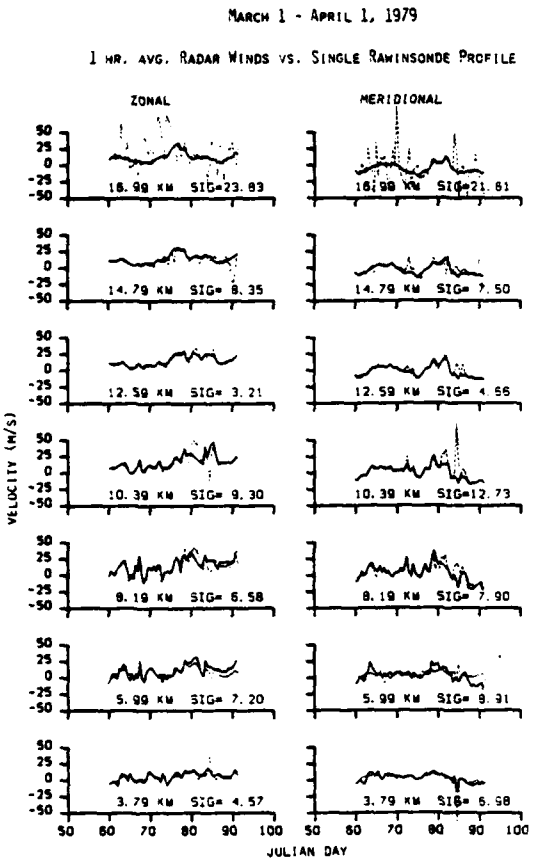

FIG. 3. Comparison of 1 h average radar winds (light dashed line) and rawinsonde wind measurements (heavy solid line) at seven successive heights during March 1979. The rms (root-mean-square) differences are shown at bottom right-hand side of each box.

component and from a minimum of 4.66 m s^{-1} to a maximum of 12.73 m s^{-1} in the meridional component. The variation of sigma with height follows the variation of the mean wind for the period as a function of height. The mean wind has been plotted in Fig. 4. Schlatter (1975) and Jasperson (1982) also found that the difference between the objectively analyzed wind and the measured wind varied as the mean wind profile.

The difference in the winds measured at the two locations with the two different techniques can be attributed to a combination of three factors. First, there are errors in the wind measurements; second, there is variability in the wind over the spatial separation between the two sites; and third, there is temporal variability. The rawinsonde takes approximately 1 h to ascend through the height range where reliable measurements can be made by the radar. The radar measurements presented here are 1 h averages, but the rawinsonde will spend only a few minutes within any one of the radars range gates.

It should be possible to decrease the rms differences between the two wind measurements by averaging the measurements over longer time intervals if some of the difference is due to small-scale temporal and spatial variability and if the winds are statistically well behaved. Indeed, that is the case. Fig. 5 shows the comparison between the 24 h average rawinsonde and radar winds. The radar average consists of 24 h of wind profiles taken every 4 min. The rawinsonde average consists of three wind profiles, one taken at either 0000 or 1200 GMT and the profile preceding and following it. The rms differences have decreased to a maximum of 6.52 m s^{-1} in the zonal component and a maximum of 7.33 m s^{-1} in the meridional component.

A comparison of the 12 h average radar winds and the winds measured by individual rawinsonde ascents was also made. In other words, the averaging interval was increased for the radar when compared to Fig. 3 but not for the rawinsonde. The rms differences still decreased significantly when compared to the case of the 1 h averages. The difference between a 1 h and a 12 h average of the radar winds was primarily that many of the large spikes in the radar data have been eliminated. The original time series shown in Fig. 1 has quite a few large spikes. Some of them are isolated, but a number of them occur during periods of high variability, indicating that they are likely to be real. Averaging decreases the large errors that arise due to this effect. The rawinsonde winds do not exhibit any of these spikes in spite of the fact that they are not averaged over long time intervals as the radar winds are. However, the profiles are routinely edited to delete wind data at any heights characterized by large changes in wind direction or wind speed over 1–2 min intervals during the ascent. An attempt was made to subject the radar data to the same type of screening. The exact

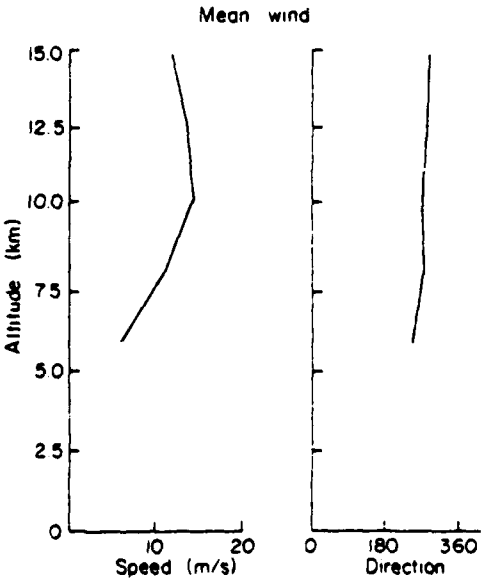

FIG. 4. Mean wind profile for the 32-day period based on the radar wind measurements. The zonal and meridional wind components were averaged separately to determine the curves.

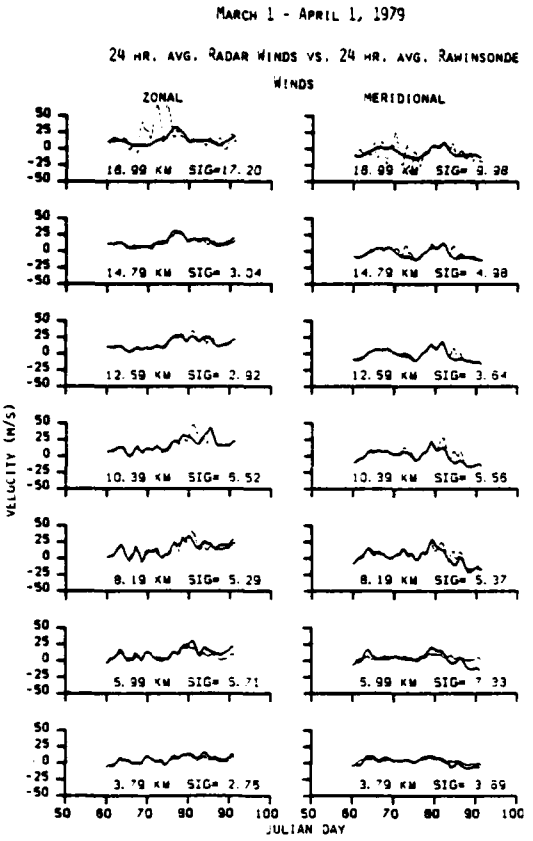

FIG. 5. Comparison of 24 h average radar winds (light dashed line) and averages of three successive rawinsonde wind measurements (heavy solid line).

criteria could not be applied since 1–2 min of balloon ascent correspond to approximately 300–600 m of altitude. The height resolution of the radar measurements is 2.2 km. Thus, the rawinsonde criteria were linearly extrapolated by multiplying the change over 600 m by the appropriate factor to get the corresponding change over 2.2 km. There is little doubt that the two procedures are not equivalent. In any case, applying the error criteria did not change the results significantly.

Figs. 3 and 5 both show a similar behavior in one respect. The agreement between the radar and rawinsonde wind measurements is quite good until day 78. After that a large discrepancy arises. One would suspect that most of the rms difference between the two measurements is attributable to the period from day 78 until the end. I will show later than the statistics are quite different for the first half and the last half of the month and discuss possible reasons for such an effect.

5. Comparison of measured winds and geostrophic winds

The Cressman analysis is an objective analysis scheme used to interpolate data from irregularly spaced grid points to a regular grid suitable for analysis or input to a numerical model. Given a series of observations f_i' where the index i ranges over the number of observations that influence the grid point, the value of f at the grid point f_g will be given by

$$f_g' = f_g^c + \sum_{i=1}^{n} C_i^f f_i'. \tag{1}$$

The quantity f_g^c is an initial guess of the value of f at the grid point. The initial value will be modified by the observed changes from the initial guesses at the observation points given by $f_i' = f_i^0 - f_i^c$. The actual observed value is f_i^0. The weighting function is given by $C_i^f = n^{-1}\cdot(R^2 - D^2)/(R^2 + D^2)$, where R is the radius of influence and D is the distance from the observation point to the grid point. The weight is zero if D is greater than R. The distance D was calculated from the formula given by Schlatter (1975)

$$D = r_E\left\{(\phi_g - \phi_i)^2 \cos^2\left[\frac{1}{2}(\theta_g + \theta_i)\right] + (\theta_g - \theta_i)^2\right\}^{1/2}, \tag{2}$$

where r_E is the radius of the earth, θ is latitude and ϕ is longitude. The form of the objective analysis scheme used here has been described in detail by Kruger (1969).

The geostrophic wind components were derived from the observed values of the geopotential height at the five radiosonde stations shown in Fig. 2. Values were interpolated to a grid with a spacing of 100 km and aligned along the north–south and east–west axes. The central grid point was positioned to coincide with the location of the Poker Flat radar. Typically, the interpolation procedure would be confined to fixed pressure surfaces. However, the radar measures the velocity at a fixed height irrespective of pressure. Thus, the initial guesses of the geopotential height at the observation points had to be derived in a slightly different way. The pressure at the height of the seven different radar ranges was calculated based on the Fairbanks sounding. The height of the corresponding pressure surface at the four surrounding radiosonde stations was calculated, and the derived height values at a given station were then averaged for the entire 30-day period during which data were available. Therefore, the initial or climatological value of the height at a given radiosonde station is the average geopotential height, for the period, of the average pressure surface corresponding to the height of the radar range gate at Poker Flat.

The 24 h average radar winds are plotted in Fig. 6 together with the geostrophic wind calculated from the height field obtained by applying the procedure described above. The rms differences are larger than those between the radar and rawinsonde wind measurements. Also, the errors are much larger in the meridional component than in the zonal component. It appears that most of the contribution to the large rms differences come from the second half of the time series. Fig. 7 is similar to Fig. 6 but shows the 24 h average

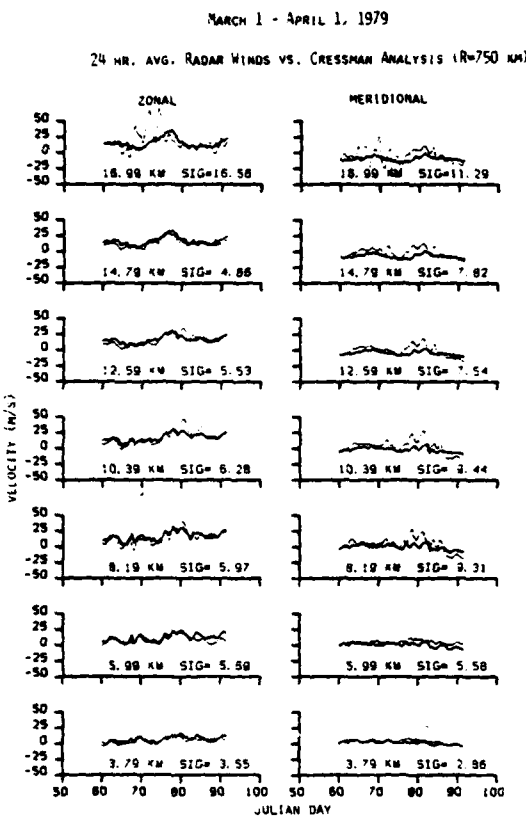

FIG. 6. Comparison of 24 h average radar winds (light dashed line) and the geostrophic wind (heavy solid line). The geostrophic wind was calculated from a grid of geopotential height values derived using the Cressman objective analysis scheme with a radius of influence of 750 km.

rawinsonde winds as opposed to the 24 h average radar winds. The rms differences between each of the wind measurements and the geostrophic winds are comparable.

The behavior of the differences between the radar winds and the geostrophic winds is summarized in Fig. 8a and 8b. The error decreases as the averaging interval is increased in both the zonal and meridional component. Although the error decreases significantly when the averaging interval is increased from 1 hour to 12 hours, particularly in the meridional component, the reduction is relatively small when the averaging interval is increased further. The error is much larger in the meridional component than in the zonal component. The overall shape of the curves is very similar to the shape of the mean wind profile shown in Fig. 4.

The rms differences between the three 24 h averages are shown in Fig. 9a for the zonal component and 9b for the meridional component. There is very little difference between the three for the zonal component, although the radar and balloon wind measurements are most similar at the two highest altitudes. The radar and balloon winds are most similar for the meridional component except at the two lowest altitudes. It appears that in general the differences between the two independent wind measurements are smaller than the differences between the measured and geostrophic winds, but the changes are so small that it is difficult to justify any inferences on the basis of these results. However, when the first and second half of the data sets are treated separately, the relationship is much clearer.

6. Comparison of first and second half of data set

Close examination of Figs. 3, 5, 6 and 7 shows that most of the contribution to the rms differences between the radar and rawinsonde winds, the radar winds and the geostrophic wind, and the rawinsonde winds and the geostrophic winds derives from the time period between day 78 and day 92, the end of the period when data are available. The time series were divided into two segments, one from 1 March to 16 March and the other from 17 March to 1 April. The rms differences were calculated for each half for 1 and 24 h averages. The large deviations occur later than 17 March, but the data set was divided in half so as not to change the statistics simply due to differences in the number of samples in each set.

Table 1 shows that all errors are comparable in the second half of the data set for both the 1 and 24 h

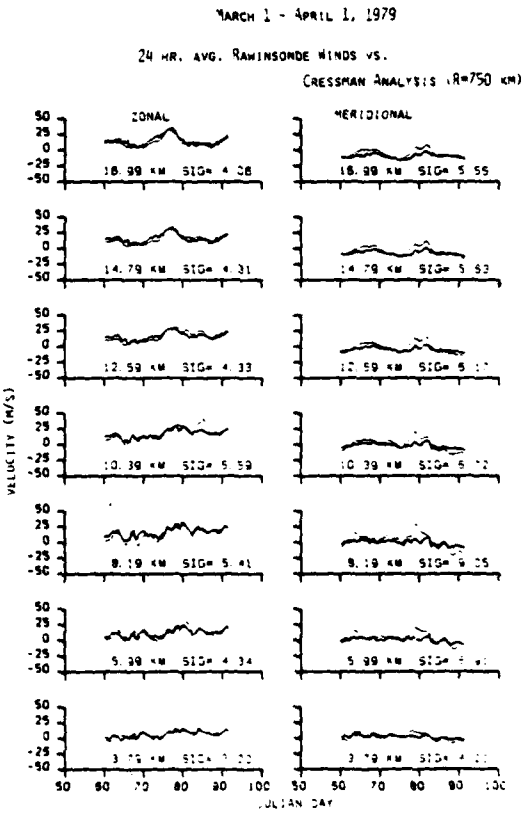

FIG. 7. As in Fig. 6 but for an average of three successive rawinsonde measurements instead of the radar wind measuremen

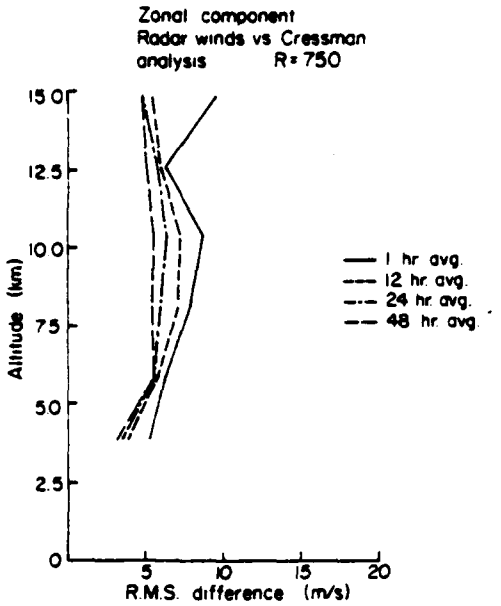

FIG. 8. (a) Summary plot of the rms differences between the zonal component of the radar winds and geostrophic winds for various averaging intervals.

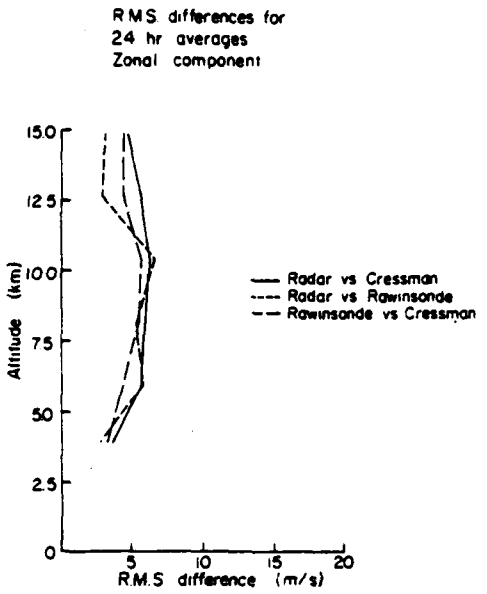

FIG. 9. (a) Summary plot of the rms differences for the radar/geostrophic wind, radar/rawinsonde and rawinsonde/geostrophic wind comparisons for the zonal component.

averages. However, the relationships that emerged when the time period was treated as a whole are much clearer in the first half. When a 1 h average of the radar data is compared to a single rawinsonde ascent, the differences are 3.19 m s^{-1} in the zonal component and 4.03 m s^{-1} in the meridional component. The differences between the radar and geostrophic winds, and the rawinsonde and geostrophic winds are nearly identical and 1.5–2.0 m s^{-1} greater than the difference between the radar and rawinsonde winds. Averaging for 24 h decreases the difference between the two independent wind measurements to 2.21 and 3.10 m s^{-1}. The difference between the measured winds and the geostrophic winds is still 1.5–2.0 m s^{-1} greater than the difference between the two wind measurements.

Fukao *et al.* (1982) compared data taken with the Arecibo 430 MHz radar and rawinsonde data from San Juan, Puerto Rico. The separation between the two sites is ~75 km. Their radar wind profiles were averages over 30 min, but their data taking scheme did not involve long-time sequences such as those in the Poker Flat data. Consequently, they could not av-

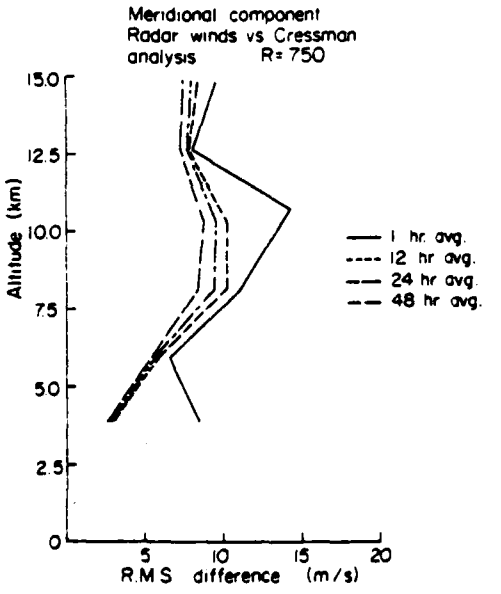

FIG. 8. (b) As in Fig. 8a but for the meridional wind component.

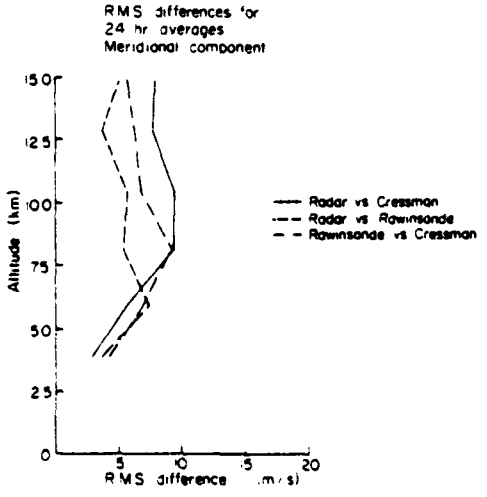

FIG. 9. (b) As in Fig. 9a but for the meridional wind component.

TABLE 1. Root mean square differences.

	3/1/79–3/16/79		3/17/79–4/1/79	
	u	*v*	*u*	*v*
1-hour averages				
Radar vs. Rawinsonde	3.19	4.03	8.45	10.70
Radar vs. Cressman Analysis	5.67	5.57	8.40	12.37
Rawinsonde vs. Cressman Analysis	6.54	5.30	6.08	8.84
24-hour averages				
Radar vs. Rawinsonde	2.21	3.10	5.59	6.44
Radar vs. Cressman Analysis	4.66	4.60	5.79	8.95
Rawinsonde vs. Cressman Analysis	5.29	4.60	5.20	8.22

erage over longer time intervals. A total of 26 separate rawinsonde ascents were used in the comparison. They found a distinct variation in the magnitude of the rms differences above and below the tropopause. The tropospheric value was 4.9 m s^{-1} and the stratospheric value was 3.3 m s^{-1}. The difference that they calculated for the stratosphere is in good agreement with the value found in this study when the 1 h averages of the radar winds were compared to single rawinsonde ascents. However, there was no indication in this study of a change in the magnitude of the differences when crossing from the troposphere into the stratosphere, although there was a variation that followed the mean wind profile.

Fukao *et al.* (1982) estimated the error of the rawinsonde measurements to be 1.9 m s^{-1} for the average conditions during their experiment although, on occasion, the error was as large as 7.1 m s^{-1} when the wind speeds were large. They attributed the differences in the stratosphere to errors in the rawinsonde measurements and the larger differences in the troposphere to a combination of the rawinsonde errors and increased variability below the tropopause. The difference between the two wind measurements in this study was found to be 3–4 m s^{-1}. However, it cannot be attributed to the error in the rawinsonde measurement since the difference between both wind measurements and the geostrophic wind was about the same, indicating that the difference is due to the spatial and temporal variability at scales comparable to the separation between the two sites and/or the averaging interval.

Jasperson (1982) studied mesoscale wind variability using a series of balloons tracked by the METRAC positioning system. He was able to study the variability at the time lags from 30 min to 5 h and spatial separations from 20 m to 20 km. Separations as large as 35 km were not studied, but Jasperson's results can be extrapolated to estimate the variability corresponding to the separation between Fairbanks and Poker Flat. The derived value is close to 3 m s^{-1} when a power law of the form given by his Eq. (1) is used together with the values that he measured at 4.415 and 20.910 km separation. That is in good agreement with the differences between the 1 h average radar winds and the rawinsonde winds in this study. Jasperson's (1982) results also suggest that the differences in the rms values characteristic of the troposphere and stratosphere found by Fukao *et al.* (1982) could be due to the effect of the changing separation between the balloons and the radar observation site above and below the tropopause. Their Fig. 1 shows the balloon trajectories for the 26 individual ascents. Due to the prevailing stratospheric easterlies during August and September at 18°N, the trajectories are such that the rawinsondes begin to approach the radar site once they get into the stratosphere. The effect of decreasing variability with decreasing spatial separation would be to decrease the difference between the two measurements.

7. Effect of varying the radius of influence

All of the curves so far have shown results for a Cressman objective analysis scheme with a radius of influence of 750 km. This particular radius was chosen because it was the optimum value when the entire height range where radar data were available was considered. Figs. 10a and 10b show the rms differences between the 24 h average radar winds and the geostrophic winds as a function of the radius of influence. The 750 km value gives the best result over all, although at the two lowest altitudes the best result is achieved when R = 1000 km. However, the difference in the errors when the larger value is used is very small below the tropopause but can amount to 1–2 m s^{-1} at the tropopause and in the lower stratosphere. A radius of influence of 750 km also gives the best result for the meridional component, but the error is much less dependent on the radius chosen in this component than in the zonal component.

The Gandin objective analysis scheme described by Kruger (1969) was also tested. The basic difference is in the weighting function. While the Cressman analysis uses a parabolic weighting function, the Gandin method uses a Gaussian weighting, and both schemes are univariate. I will not present the results in graphic form since the difference in all cases was only a fraction of a meter per second, less than the accuracy of the radar measurements during the spring of 1979.

The Cressman analysis is often applied in a series of successive scans (Cressman, 1959; Otto-Bliesner *et al.*, 1977). A large radius of influence is chosen initially so as to include information from many stations surrounding the grid point. The radius is then decreased successively, until finally only the nearest stations affect the analyzed value. The successive scans method was also applied to the Alaska radiosonde data. The initial radius was 2000 km, and it was decreased by 400 km in each of four successive passes through the data. The result of this analysis was actually worse than the single scan with a radius of 750 km. The average difference

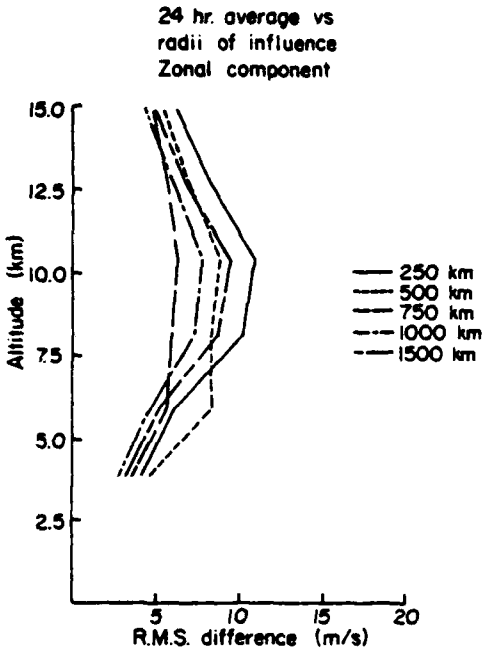

FIG. 10. (a) Differences between the 24 h average radar winds and the geostrophic winds for various radii of influence for the zonal wind component.

in the rms error was slightly greater than 1 m s^{-1}. The successive scans method produced more variability in the geostrophic winds calculated from the analyzed geopotential height fields, but the short-term variations did not improve the agreement with the radar or rawinsonde winds.

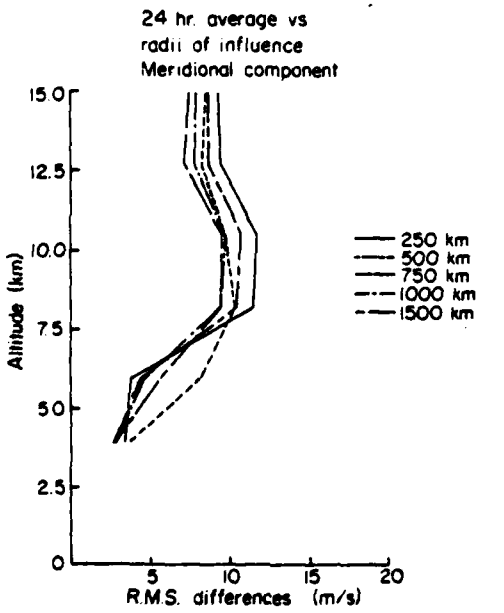

FIG. 10. (b) As in Fig. 10a but for the meridional component.

8. Correlation between winds and geopotential heights

The correlation coefficients between the zonal winds and geopotential heights are plotted in Fig. 11. Multivariate objective analysis schemes such as those of Schlatter (1975), Rutherford (1972) and Bergman (1979) carry out the objective analysis procedure based on both height and wind data. The wind information supplements the observed height field data when the two quantities are related through the geostrophic relation. The procedure, in effect, assumes that the correlation between the height fields and the winds is unity at zero spatial separation. Fig. 11 shows the correlation coefficient for a 24 h average wind to be nearly independent of height with a value of approximately 0.75.

Since the statistics for the rms differences are clearly very different for the first and second half of the data sets, the correlation coefficients were also calculated separately for each half. The results are shown in Table 2. The correlations are nearly identical in both halves, unlike the situation for the rms differences. When the averaging interval is increased from 1 to 24 h, the correlations increase for both the radar/rawinsonde comparison and the radar/geostrophic wind comparison. The same is not true for the rawinsonde/geostrophic wind comparison. The correlation coefficients are virtually identical for the 1 h average, i.e., single profile, and 24 h average, i.e., three-profile comparisons. Again, the filtering applied to the height variations in the balloon wind measurements is a possible explanation for this result.

9. Comparison with earlier results

Most previous estimates of the synoptic error of the rawinsonde wind measurements have involved com-

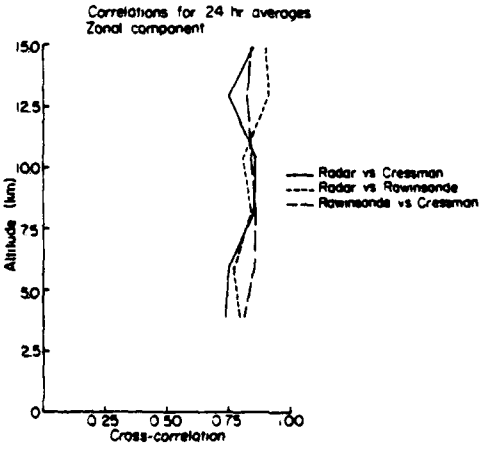

FIG. 11. Cross correlation between the 24 h average radar and geostrophic winds, between the radar and rawinsonde winds, and between averages of three successive rawinsonde measurements and the geostrophic winds. The correlations are for the zonal wind component. Values for the meridional component are similar.

TABLE 2. Cross correlations.

	3/1/79–3/16/79		3/17/79–4/1/79	
	u	*v*	*u*	*v*
1-hour averages				
Radar vs. Rawinsonde	0.541	0.529	0.522	0.550
Radar vs. Cressman Analysis	0.589	0.470	0.545	0.504
Rawinsonde vs. Cressman Analysis	0.661	0.734	0.676	0.829
24-hour averages				
Radar vs. Rawinsonde	0.768	0.712	0.702	0.834
Radar vs. Cressman Analysis	0.700	0.503	0.682	0.685
Rawinsonde vs. Cressman Analysis	0.691	0.731	0.712	0.826

parisons of observed values and the output grid values from numerical models or objective analysis procedures (e.g., Lyne *et al.*, 1982; Bergman, 1979; Bengtsson *et al.*, 1982). Such an approach was necessitated by the lack of another routine measurement technique with accuracy comparable to the rawinsonde measurement as shown by Bengtsson *et al.* (1982) who present a summary of the estimated accuracies of the various wind measurements used operationally. Also, the comparison between observations and objective analysis or model output is of direct interest since it provides a direct estimate of the magnitude of the unbalanced wind component in the observations.

Lyne *et al.* (1982) found the difference to be between 3 m s^{-1} at low levels and 4 m s^{-1} at high levels near 100 mb. Their results are roughly consistent with, though smaller than, the range of 2–6 m s^{-1} given by Bengtsson *et al.* (1982). Both sets of differences are much smaller than the best case estimate of 7.98 m s^{-1} at 500 mb calculated by Bergman (1979). However, the latter was based on assumed values for the magnitude of the errors that are needed for the optimum interpolation objective analysis scheme. The differences found in this study by direct comparison of the balloon and radar measurements were 3.19 m s^{-1} for the zonal component and 4.03 m s^{-1} for the meridional component, in good agreement with the results of Lyne *et al.* (1982).

Although the differences between the two wind measurements are likely due to small-scale spatial and temporal variability, the fact that the difference between the measured winds and the geostrophic winds remains nearly constant as the averaging interval is increased indicates that there is a contribution to the variance from an ageostrophic wind component. The rms value of the ageostrophic wind component based on the differences given in Table 1 would be approximately 1.5–2.0 m s^{-1}. This study has dealt with only one site and the result may be linked to the location and local orography. It may be possible, however, to sort out such effects in the future by using the Poker Flat data sets that include both the horizontal and vertical wind components.

Table 1 shows that there is a clear difference between the first half of the period studied and the second half. In the first half, the two wind measurements are very similar and the estimate of the ageostrophic wind component is the same based on both techniques. In the second half, the differences between the radar and balloon wind measurements are much larger than in the first half and the difference between the measured and geostrophic winds is about the same as the difference between the two independent wind measurements. The data processing for the radar data did not change in any way during the month and none of the radar components such as transmitters or receivers were modified or failed during this period. Thus, there is no reason to expect a deterioration in the quality of the radar data. Also, the comparisons involving the balloon measurements are as poor at this time as those involving the radar. I have examined the 500 mb charts for the entire period, but there were no fundamental differences in the overall flow pattern during the first and second half of the month. One difference that is evident in Fig. 1 is the amount of short-term variability in the radar data after the time labeled 600 h. Aside from the episode of very large and rapid variations at 720 h, there is also consistently more variability overall. Table 3 shows the variance of the radar winds at each height for the first and second half of the period and supports this conclusion. It is clear that the amount of power in small time-scale variability increases in the second half of the period, although the cause is not clear and will have to be investigated further.

10. Conclusion

This study has shown that a VHF radar operated continuously in a mode such as the Poker Flat MST radar can provide synoptically meaningful data. Comparison of the radar wind measurements and radiosonde pressure and wind data has made it possible to assess the representativeness of the radar data directly. Differences between the radar and balloon wind measurements were explained by the wind variability over the distance separating the two measurements sites. As the averaging interval was increased, the differences decreased.

If the radar data are used in the future for synoptic applications, the data will either have to be averaged

TABLE 3. Variances of radar winds.

	3/1/79–3/16/79		3/17/79–4/1/79	
	u	*v*	*u*	*v*
3.79 km	4.40	2.49	5.89	8.24
5.99 km	4.88	2.89	7.44	6.36
8.19 km	8.67	6.10	11.39	16.72
10.39 km	6.63	6.15	11.51	16.40
12.59 km	5.14	5.75	8.39	13.04
14.79 km	7.96	9.79	10.05	12.78

temporally over some period appropriate to the numerical model that is used or a vertical variation filter such as that applied to the rawinsonde data will have to be used. The results of this study will help in designing criteria for the former case. The latter case could not be investigated using Poker Flat data that are presently available since the height resolution is too coarse to apply the empirical rawinsonde filters.

The data set studied here was the first long time series of horizontal winds produced by the Poker Flat radar. Beginning in the early part of 1981, the radar continuously measured all three wind components simultaneously. The longer data set should be used to check the preliminary results presented here, including the possibility of changes in the short-term variability. Finally, the same types of comparisons should be carried out with some of the better objective analysis schemes that are now available. In particular, the normal mode method has many advantages in that it not only produces analyzed fields that are exactly consistent with a given numerical model, but it can also be used to determine the contributions from the fast (gravity wave) and slow (inertio-gravity and Rossby wave) components of the geopotential and velocity fields separately. Also, the normal mode analysis does not impose the constraint of geostrophy.

The radar measurements have been shown to produce data of a quality that is at least comparable to the earlier estimates of the representativeness of the rawinsonde winds when the radar data are averaged for an hour or more. Of course, that is not the limit of the usefulness of the radar data since it can routinely provide 1 h or even higher time resolution data. Such a capability will become increasingly useful as the smallest scales resolved by numerical models decreases further.

Acknowledgments. I am grateful to Ben B. Balsley, Dave Carter and Warner Ecklund of the Aeronomy Laboratory at NOAA for many useful discussions concerning the radar data, and particularly to Tony Riddle for generating data tapes in a convenient format and for answering many questions about the data processing. This research was sponsored by the Air Force Office of Scientific Research under Grant AFOSR-80-0020.

REFERENCES

Balsley, B. B., and K. S. Gage, 1982: On the use of radars for operational wind profiling. *Bull. Amer. Meteor. Soc.*, **63**, 1009–1018.

——, W. L. Ecklund, D. A. Carter and P. E. Johnston, 1980: The MST radar in Poker Flat, Alaska. *Radio Sci.*, **15**, 213–224.

Bengtsson, L., M. Ghil and E. Kallen, Eds., 1981: *Dynamic Meteorology: Data Assimilation Methods. Applied Mathematical Sciences Series*, Vol. 36. Springer-Verlag, 330 pp.

——, M. Kanamitsu, P. Kallberg and S. Uppala, 1982: FGGE 4-dimensional data assimilation at ECMWF. *Bull. Amer. Meteor. Soc.*, **63**, 29–43.

Bergman, K. H., 1979: Multivariate analysis of temperature and winds using optimum interpolation. *Mon. Wea. Rev.*, **107**, 1423–1444.

Carlson, H. C., Jr., and N. Sundararaman, 1982: Real-time jetstream tracking: National benefit from an ST radar network for measuring atmospheric motions. *Bull. Amer. Meteor. Soc.*, **63**, 1019–1026.

Cressman, G. P., 1959: An operational objective analysis system. *Mon. Wea. Rev.*, **87**, 367–374.

Daley, R., 1981: Normal mode initialization. *Rev. Geophys. Space Phys.*, **19**, 450–468.

Fukao, S., T. Sato, N. Yamasaki, R. M. Harper and S. Kato, 1982: Winds measured by a UHF Doppler radar and rawinsondes: Comparisons made on twenty-six days (August–September 1977) at Arecibo, Puerto Rico. *J. Appl. Meteor.*, **21**, 1357–1363.

Gage, K. S., and B. B. Balsley, 1978: Doppler radar probing of the clear atmosphere. *Bull. Amer. Meteor. Soc.*, **59**, 1074–1093.

Harper, R. M., and W. E. Gordon, 1980: A review of radar studies of the middle atmosphere. *Radio Sci.*, **15**, 195–211.

Hogg, D. C., F. O. Guiraud, C. G. Little, R. G. Strauch, M. T. Decker and E. R. Westwater, 1980: Design of a ground-based remote sensing system using radio wavelengths to profile lower atmospheric winds, temperature, and humidity. *Remote Sensing of Atmospheres and Oceans*. Academic Press, 313–364.

Jasperson, W. H., 1982: Mesoscale time and space wind variability. *J. Appl. Meteor.*, **21**, 831–839.

Kruger, H. B., 1969: General and special approaches to the problem of objective analysis of meteorological variables. *Quart. J. Roy. Meteor. Soc.*, **95**, 21–39.

Larsen, M. F., and J. Röttger, 1982: VHF and UHF Doppler radars as tools for synoptic research. *Bull. Amer. Meteor. Soc.*, **63**, 996–1008.

——, M. C. Kelley and K. S. Gage, 1982: Turbulence spectra in the upper troposphere and lower stratosphere at periods between 2 hours and 40 days. *J. Atmos. Sci.*, **39**, 1035–1041.

Lorenc, A. C., 1981: A global three-dimensional multivariate statistical interpolation scheme. *Mon. Wea. Rev.*, **109**, 701–721.

Lyne, W. H., R. Swinbank and N. T. Birch, 1982: A data assimilation experiment and the global circulation during the FGGE special observing periods. *Quart. J. Roy. Meteor. Soc.*, **108**, 575–594.

Otto-Bliesner, B., D. P. Baumhefner, T. W. Schlatter and R. Bleck, 1977: A comparison of several meteorological analysis schemes over a data-rich region. *Mon. Wea. Rev.*, **105**, 1083–1091.

Röttger, J., 1980: Structure and dynamics of the stratosphere and mesosphere revealed by VHF radar investigations. *Pure. Appl. Geophys.*, **118**, 494–527.

Rutherford, I. D., 1972: Data assimilation by statistical interpolation of forecast error fields. *J. Atmos. Sci.*, **29**, 809–815.

Sato, T., and S. Fukao, 1982: Altitude smearing due to instrumental resolution in MST radar measurements. *Geophys. Res. Lett.*, **9**, 72–75.

Schlatter, T. W., 1975: Some experiments with a multivariate statistical objective analysis scheme. *Mon. Wea. Rev.*, **103**, 246–257.

——, G. W. Branstator and L. G. Thiel, 1976: Testing a global multivariate statistical objective analysis scheme with observed data. *Mon. Wea. Rev.*, **104**, 765–783.

Strauch, R. G., 1981: Radar measurement of tropospheric wind profiles. *Preprints 20th Conf. Radar Meteorology*. Boston, Amer. Meteor. Soc., 430–434.

——, M. T. Decker and D. C. Hogg, 1982: An automatic profiler of the troposphere. *Preprints AIAA 20th Aerospace Sciences Meeting*. Orlando, Amer. Inst. Aeronaut. Astronaut. No. AI44-82-0014.

Woodman, R. F., and A. Guillen, 1974: Radar observations of winds and turbulence in the stratosphere and mesosphere. *J. Atmos. Sci.*, **31**, 493–505.

15.4

Conference Volume: 22nd Conference On Radar Meteorology, 10-13 Sept. 1984, Zurich, Switzerland. Published By The Amer. Meteorological Society, Boston, Mass. USA

OBSERVATIONS OF FRONTAL ZONE STRUCTURES

WITH A VHF DOPPLER RADAR AND RADIOSONDES

M. F. Larsen

Cornell University
Ithaca, NY 14853

and

J. Röttger

EISCAT Scientific Association
Kiruna, Sweden

1. INTRODUCTION

The SOUSY-VHF-Radar is a pulsed coherent radar operating at 53.5 MHz and located near Bad Lauterberg, West Germany. Since 1977, the facility, operated by the Max-Planck-Institut für Aeronomie, has been used to make a series of frontal passage observations in the spring and fall. Experiments in winter have been difficult because part of the transmitting and receiving array is usually covered by snow during that part of the year. Wavelengths around 6 m are known to be sensitive to the vertical temperature structure of the atmosphere (Green and Gage, 1980; Rastogi and Röttger, 1982). Thus, it has been possible to use radars operating at frequencies near 50 MHz to locate the tropopause. Comparisons between radar data and radiosonde data have shown that there is a large gradient in the radar reflectivity at the height where the radiosonde tropopause occurs.

An experiment carried out by Röttger (1979) on March 15-16, 1977, showed that the radar's sensitivity to the vertical temperature structure could also be used to locate the position of fronts. The SOUSY-VHF-Radar consists of a transmitting array, also used for receiving in some configurations, that can be scanned in the off-vertical direction but not at sufficiently low elevation angles to study the horizontal extent of structures as extended as fronts. Gage and Balsley (1978), Balsley and Gage (1980), Röttger (1980), and Larsen and Röttger (1982) have reviewed UHF and VHF Doppler radar techniques and applications to atmospheric research. In the experiments described here, the radar was operated in the spaced antenna mode. Röttger and Vincent (1978) and Vincent and Röttger (1980) have described the method and its advantages. The transmitting array consists of 196 Yagi antennas, and the receivers are three separate arrays of 32 Yagis each. The effective antenna aperture was 2500 m^2, the applied average transmitter power was typically 20 KW, and the height resolution was 150 m. Vertical profiles of the reflectivity were obtained in each of the three receiver arrays, and it was found that besides the enhancement of the signal strength associated with the tropopause region, there was also a secondary band of enhanced reflectivities stretching downward from the upper to the lower troposphere. Comparisons between the radar data and data from a nearby radiosonde station show that the band is associated with the temperature gradients in a passing frontal zone. The vertical and horizontal velocities were also measured during the experiments, but they will not be discussed here.

The results of analyzing two events have been presented by Röttger (1979, 1981), Röttger and

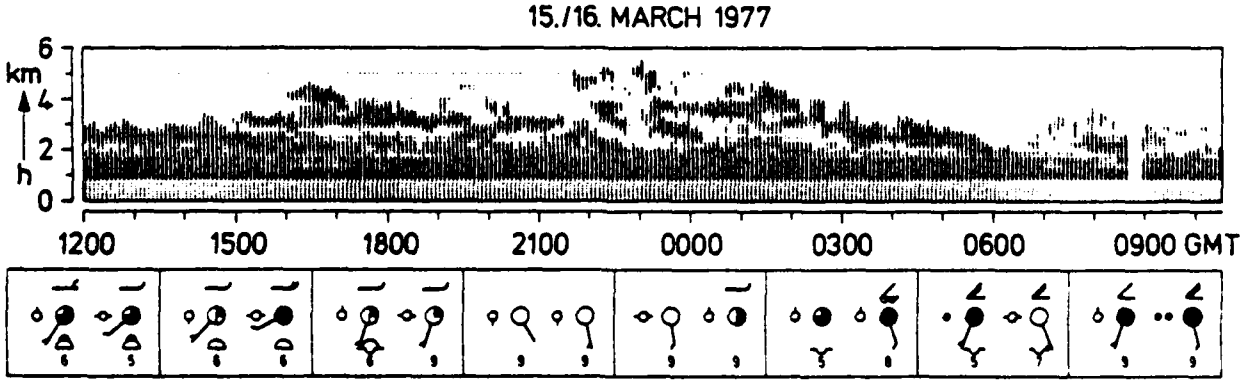

Fig. 1. Radar reflectivities as a function of height and time measured by the SOUSY-VHF-Radar. Observations from the meteorological observatories at Kassel, 60 km southwest, and Hannover, 90 km north-northwest, are shown on the left and right sides of the boxes, respectively.

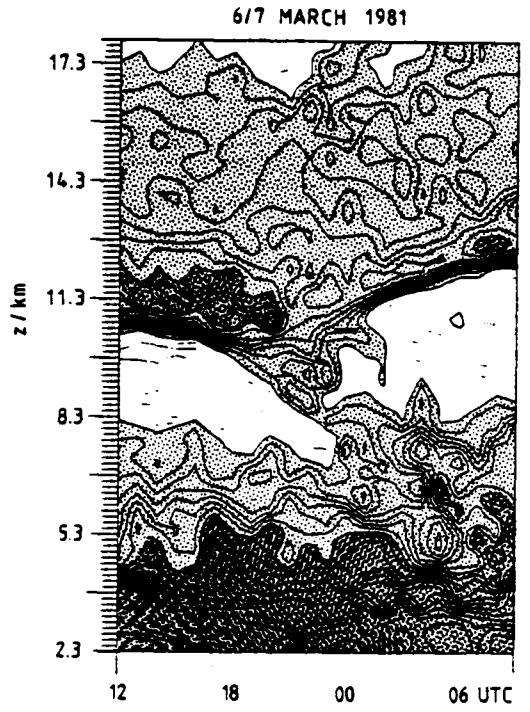

Fig. 2. Radar reflectivities as a function of height and time. Contour interval is 2 dB. Stippled areas show higher reflectivities.

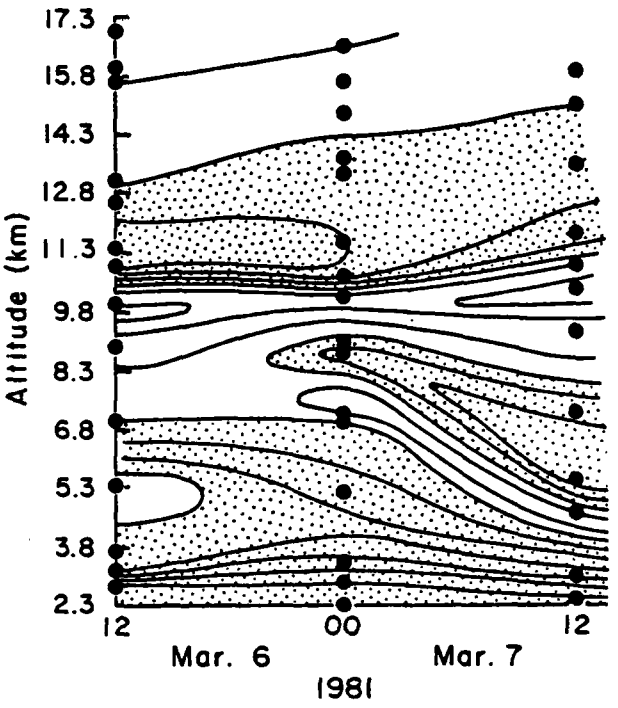

Fig. 3. Gradient of potential refractive index calculated from Hannover radiosonde data for the time period corresponding to the reflectivities shown in Figure 2. Stippled areas correspond to larger values.

Schmidt (1981), and Larsen and Röttger (1983). However, in this paper we would like to summarize a more complete data set consisting of a series of five observations of frontal structure made with the SOUSY-VHF-Radar in March 1977, March 1981, November 1981, February 1982, and April 1984. The extensive data set shows results essentially in agreement with the preliminary results. Comparison of time/height cross sections of reflectivity measured with the radar and potential refractivity gradients calculated from radiosonde data taken at a nearby location show good agreement. Therefore, we conclude that the radar is detecting the temperature structure associated with the front and that the enhancement in reflectivities is not due to precipitation or other very localized processes. Also, we have found that the radar can be used to locate the fronts consistently, even in some cases when the fronts are rather weak.

2. March 15-16, 1977

At 0000 UTC on March 15, 1977, a low pressure center in the North Atlantic was propagating eastward toward the British Isles. The associated warm front and the trailing cold front extended southward from the center of the low. The warm front at the surface had traversed France and West Germany by 0000 UTC on March 17. Reflectivities measured with the SOUSY-VHF-Radar from 1200 UTC on March 15 to 0900 UTC on March 16 are shown in Figure 1. Cloud cover observations from two nearby meteorological observatories are shown below the reflectivities.

Of paticular interest is the band of enhanced echoes stretching from 4 km altitude at 0000 UTC on March 16 to 2 km altitude at 0600 UTC. Extrapolating the slope of the band to the surface gave a time for the surface frontal passage in agreement with that derived from the weather charts. Comparison between the temperature cross section perpendicular to the front and the features seen in the radar reflectivity data showed good agreement.

3. March 6-7, 1981

Figure 2 shows the reflectivities observed with the radar between 1200 UTC on March 6 and 0900 UTC on March 7, 1981. The contour interval is 2 dB, and the stippling indicates regions of higher reflectivity. The signal strength generally decreases with height in the troposphere but increases by 10-12 dB over a vertical distance of 0.5 km or so at the tropopause. The tropopause determinations from Hannover radiosonde data is shown by the heavy bars in the figure. The bar corresponding to 0900 UTC was actually obtainded at 1200 UTC, the standard synoptic time.

The feature of particular interest is the band of enhanced echo strength stretching downward from the tropopause beginning at approximately 1700 UTC. The feature is associated with a warm front that was essentially parallel to the

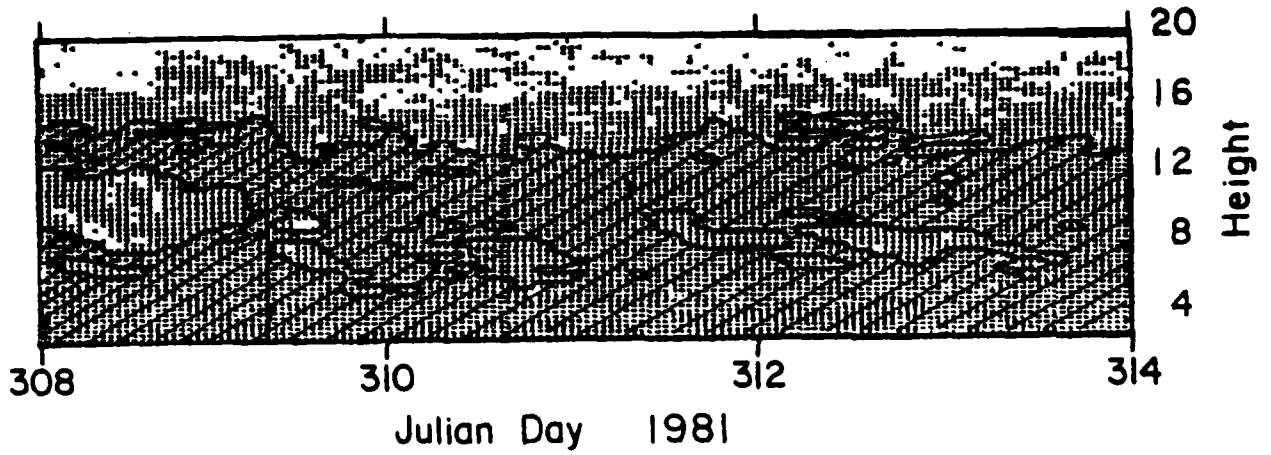

Fig. 4. Reflectivities measured by the SOUSY-VHF-Radar during the period from Nov. 4 to 10, 1981.

NNW-SSE direction and propagated eastward across West Germany and past the radar. The radar reflectivity is proportional to M^2 with M given by

$$M = -77.6 \times 10^{-6} \frac{P}{T} \left\{\frac{\partial \ln\theta}{\partial z}\right\} \cdot \left\{1 + \frac{15500}{T}\left(1 - \frac{1}{2}\frac{\partial \ln q/\partial z}{\partial \ln\theta/\partial z}\right)\right\} \qquad (1)$$

where P is in millibars, T is absolute temperature, θ is potential temperature, and q is the specific humidity. The contours of M^2 calculated from the Hannover radiosonde data are shown in Figure 3 with a contour interval of 4 dB. Once again, the stippled areas correspond to higher values. The agreement between the observations and the calculated values is quite good. The contours of M^2 show the increase in the height of the tropopause at 1200 UTC on March 7. Also, the enhancement of the echoes between 6.8 and 8.3 km after 0000 UTC on March 7 is apparent. There is an indication of the frontal echo band in the values of the potential refractivity at 0000 UTC as shown by the feature near 8.75 km altitude. However, the time resolution of the radiosonde data is not sufficient to show the details of the frontal zone structure.

4. November 4-10, 1981

In the first half of November 1981 observations were made over a period of more than a week. The reflectivities for the period from November 4 (Day 308) to November 10 (Day 314) are shown in Figure 4. On Day 308, the reflectivities decrease with altitude in the troposphere and then begin to increase just below the tropopause. A cold frontal band is observed after 1600 UTC and stretches upward in altitude with time as would be expected. Two warm frontal bands are evident as enhanced reflectivity regions moving downward with time. The first is observed near the tropopause at 0000 UTC on Day 309. The second is first seen at 0600 UTC on Day 310.

Potential temperatures were calculated from the Hannover radiosonde data and have been plotted and contoured on a scale similar to that used for the reflectivities. The results are shown in Figure 5. The same general features are evident in both figures. The packing of the potential temperature contours is characteristic of the tropopause and stratosphere. The lower boundary of the packing is located at the same height as the increase in the radar reflectivities associated with the tropopause. The cold front and the

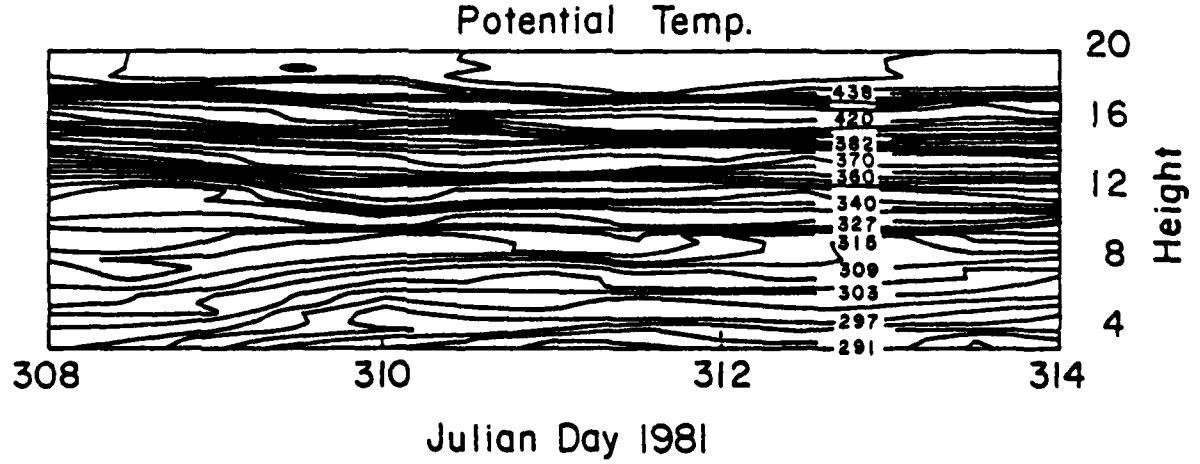

Fig. 5. Potential temperatures calculated from the Hannover radiosonde data for the period corresponding to the radar reflectivities shown in Figure 4.

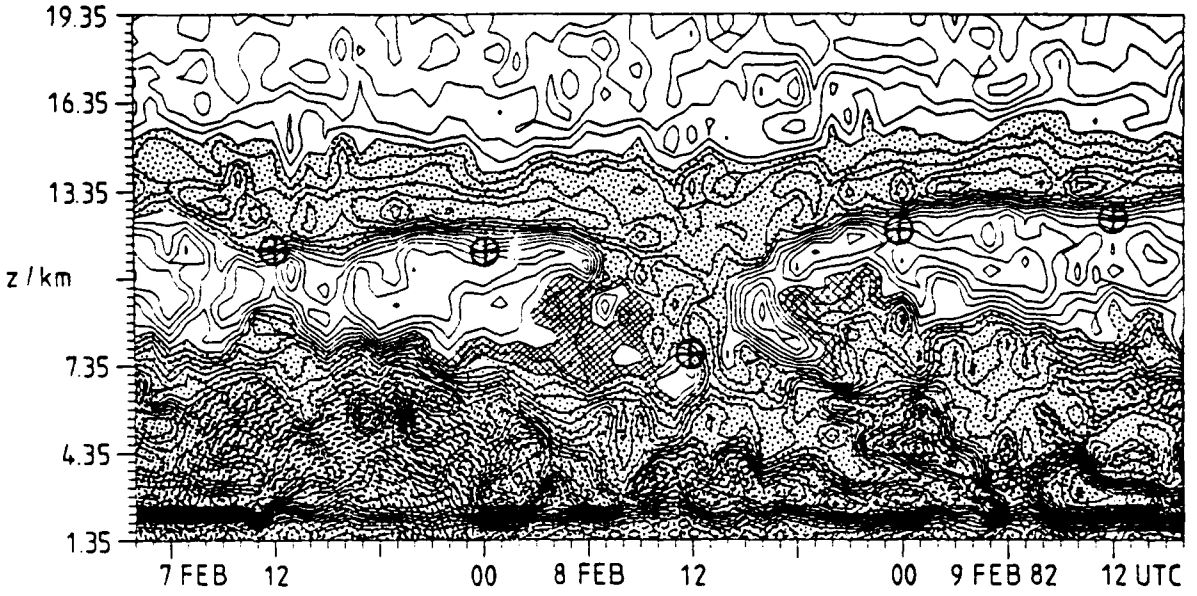

Fig. 6. Same as Figure 2 but for Feb. 7-9, 1982.

second warm front show up clearly in the potential temperature data, but the first warm frontal band is not as clearly evident. However, satellite photos for this time show two distinct cloud bands.

During the time form Nov. 4 to 10, the radar site was in a region of northerly flow on the eastern side of a stationary high pressure system centered over the British Isles. The fronts that traversed the radar site were confined to the upper troposphere, as the potential temperature cross section shows.

5. February 7-9, 1982

The reflectivities measured by the radar during the period from February 7 to 9, 1982, are shown in Figure 6. Once again the stippled areas represent larger reflectivities. However, this time the intermediate values have been cross hatched, as well. The typical features already noted in the previous examples are present. The echo strength decreases with altitude in the troposphere, but there is an enhancement in the reflectivities in the upper troposphere associated with the temperature discontinuity that defines the location of the tropopause. The heavy

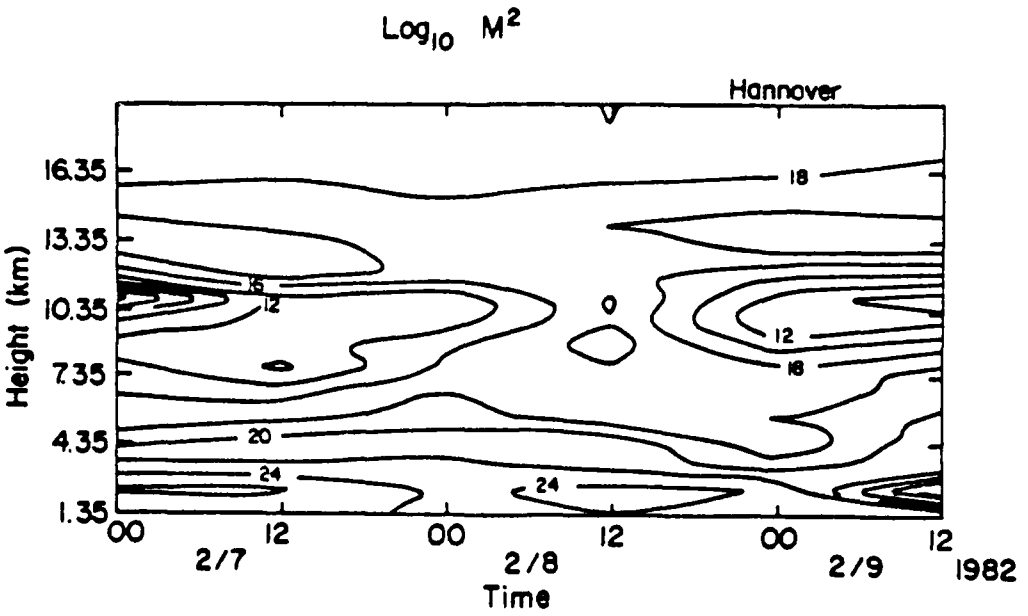

Fig. 7. Same as Figure 3 but corresponding to the data shown in Figure 6.

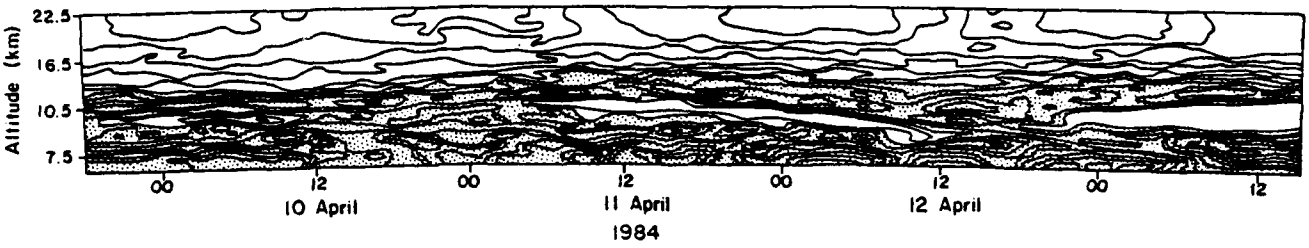

Fig. 8. Same as in Figure 2 but for the period April 9-13, 1984.

circles show the tropopause height determined from the Hannover radiosonde.

Near 1200 UTC on February 8, a band of enhanced reflectivities associated with a warm front stretches downward from the tropopause. Beginning at approximately 0200 UTC on February 8, a band of intermediate reflectivities stretches upward in connection with a cold front associated with the low pressure system. The cold front for this particular event was much weaker than the warm front, and the difference in strength accounts for the difference in the magnitude of the reflectivities.

We have also calculated the potential refractive index gradient M^2 based on Hannover radiosonde data. The vertical time section is shown in Figure 7. The same features are evident in both the reflectivity and M^2 cross sections. More detailed analysis of the event is given by Larsen and Röttger (1983).

6. April 9-13, 1984

Observations were made with the SOUSY-VHF-Radar over a five day period in April 1984. From 1200 UTC on April 9 until 1200 UTC on April 11, the radar was located in a region of northerly flow on the eastern side of a stationary high pressure system. During this time a number of mesoscale disturbances with horizontal scales of 50 to 100 km developed in the region. Most did not pass the radar, but one such system was observed near 0000 UTC on April 11. The radar reflectivities are shown in Figure 8.

The signal strength showed an enhancement in the upper troposphere during the passage of the mesoscale system, but the feature is not as narrow and does not show the tilt characteristic of the other frontal passage observations that we have presented. Late in the day on April 12 a surface frontal passage took place, as shown by the weather charts and satellite photographs. The features typical of a frontal passage are clearly present in the reflectivity data beginning at about 1600 UTC on April 11. A band of enhanced echoes begins to descend from the height of the tropopause and stretches downward toward the surface. The air mass following the frontal passage then has a higher tropopause height than the air mass prior to the frontal passage. The morphology in this event is very similar to the morphology in the other four events presented here.

7. Conclusion

Observations of five separate frontal passage events made with the SOUSY-VHF-Radar have shown that a radar operating at a frequency near 50 MHz can be used to detect the location of fronts on a routine basis. The SOUSY-VHF-Radar does not operate on a continuous basis. While the observation periods were chosen on the basis that it would be likely that a frontal passage would take place at the location of the radar, no attempt was made to choose only the strongest or most developed fronts. In fact, the front observed in April 1984 and the cold front observed in February 1982 did not have particularly strong temperature gradients.

The comparison between radar and radiosonde data have shown good agreement, indicating that the features seen in the radar reflectivity data are characteristic of the frontal temperature structure and are not associated with precipitation or local convection. That is particular true since the separation between the radar site and the nearest radiosonde station is approximately 90 km.

REFERENCES

Balsley, B. B., and K. S. Gage, 1980: The MST radar technique: Potential for middle atmospheric studies. Pure Appl. Geophys., 118, 452-493.

Gage, K. S., and B. B. Balsley, 1978: Doppler radar probing of the clear atmosphere. Bull. Am. Meteorol. Soc., 59, 1074-1093.

Green, J. L., and K. S. Gage, 1980: Observations of stable layers in the troposphere and stratosphere using VHF radar. Radio Sci., 15, 395-406.

Larsen, M. F., and J. Röttger, 1982: VHF and UHF Doppler radars as tools for synoptic research. Bull. Am. Meteorol. Soc., 63, 996-1008.

Larsen, M. F., and J. Röttger, 1983: Comparison of tropopause height and frontal boundary locations based on radar and radiosonde data. Geophys. Res. Lett., 10, 325-328.

Rastogi, P. K., and J. Röttger, 1982: VHF radar observations of coherent reflections in the vicinity of the tropopause. J. Atmos. Terr. Phys., 44, 461-469.

Röttger, J., 1979: VHF radar observations of a frontal passage. J. Appl. Meteorol., 18, 85-91.

Röttger, J., 1980: Structure and dynamics of the stratosphere and mesosphere revealed by VHF

radar investigations. Pure Appl. Geophys., 118, 494-527.

Röttger, J., 1981: The capabilities of VHF radars for meteorological observations. Proc. IAMAP Symposium, Hamburg, Aug. 25-28, 1981, European Space Agency, ESA-SP-165, Paris, France.

Röttger, J., and G. Schmidt, 1981: Characteristics of frontal zones determined from spaced antenna VHF radar observations. Preprint Volume: 20th Conference on Radar Meteorology, Nov. 30-Dec. 3, 1981, Boston, Mass., AMS, Boston, Mass.

Röttger, J., and R. A. Vincent, 1978: VHF radar studies of tropospheric velocities and irregularities using spaced antenna techniques. Geophys. Res. Lett., 5, 917-920.

Vincent, R. A., and J. Röttger, 1980: Spaced antenna VHF radar observations of tropospheric velocities and irregularities. Radio Sci., 15, 319-335.

1985 AGU SPRING MEETING

Baltimore, Maryland • May 27–May 31

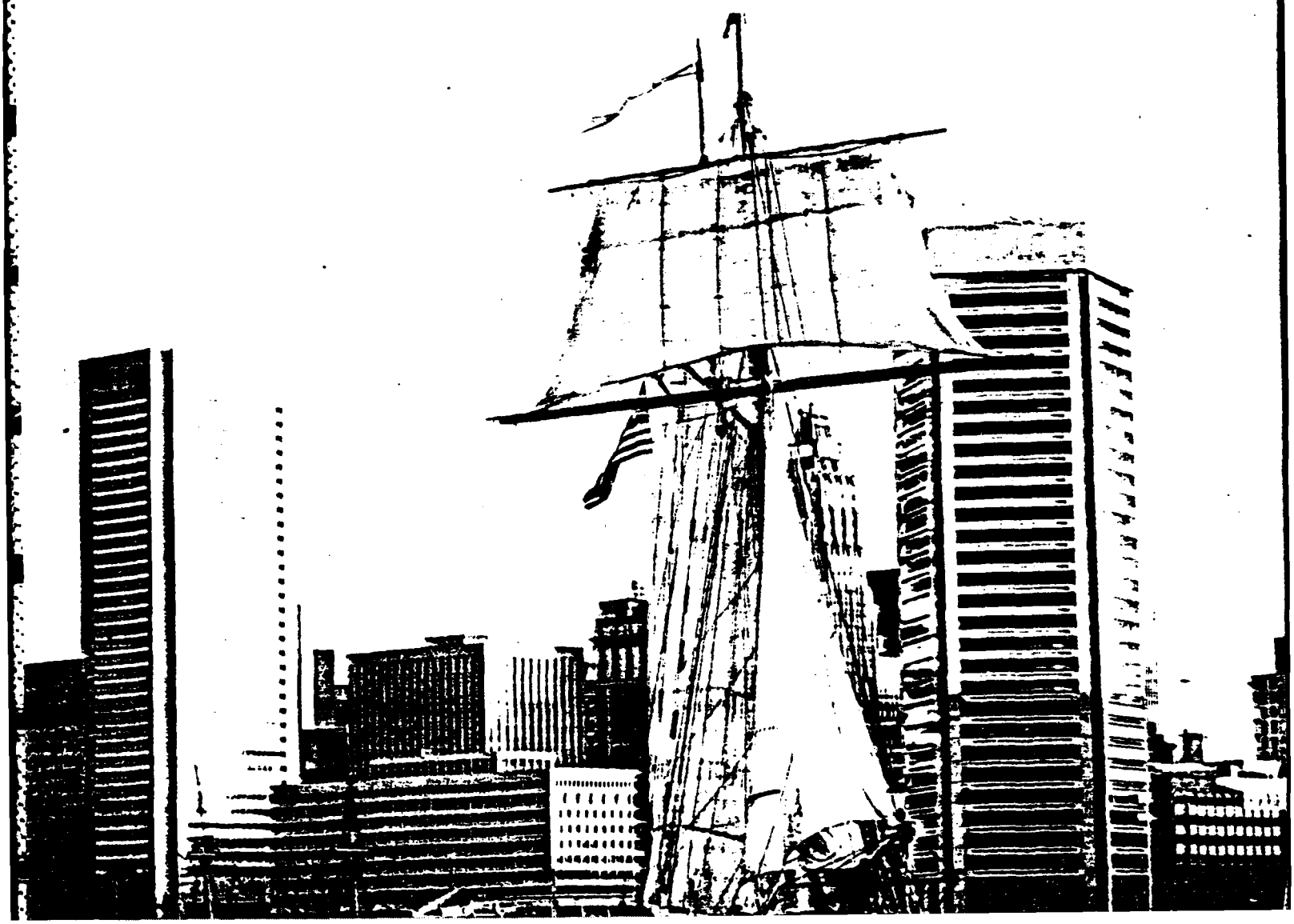

VHF-Radar Observations of Frontal Zone Structure

M. F. Larsen (Dept. of Physics and Astronomy, Clemson University, Clemson, SC 29631) and J. Rottger (Arecibo Observatory, P. O. Box 995, Arecibo, PR 00612)

Since March 1977, the SOUSY-VHF-Radar has been used to make a series of frontal passage observations in the spring and fall. The radar operates at a wavelength of 5.6 m and, thus, is sensitive to the temperature structure of the atmosphere. It has already been shown, for instance, that a VHF radar can be used to determine the location of the tropopause. We present data from five separate experiments showing that the reflectivity data can also be used to determine the location of tropopause breaks and frontal boundaries between the surface and the tropopause. In each case, we compare reflectivities measured with the radar and the potential refractivity gradient calculated from radiosonde data from a station 90 km away. There is good agreement between the calculated and observed values, although the radar data show more of the detailed structure due to the much higher time resolution.

1. 1985 Spring Meeting
2. 003362836
3. (a) M. F. Larsen
   Dept. of Physics and Astronomy
   Clemson University
   Clemson, SC 29631

   (b) 803-656-3417
4. A
5. Special Session: Application of Advanced Technology in the Atmospheric Sciences
6. O
7. 20% at 1984 Conference on Radar Meteorology
8. Bill to:
   Dept. of Physics and Astronomy
   117 Kinard Laboratory
   Clemson University
   Clemson, SC 29631
9. C

This abstract describes some of the later work supported by AFOSR-83-100. The paper has not been delivered, in fact, but the work summarized here will be the basis for a future publication.

Short Abstract

OBSERVATIONS OF MESOSCALE WAVE STRUCTURE WITH A VHF DOPPLER RADAR

M. F. Larsen[1] and J. Rottger[2]

[1]Dept. of Physics and Astronomy
Clemson University
Clemson, SC 29631

[2]Arecibo Observatory
P. O. Box 995
Arecibo, PR 00612

Abstract. In November 1981 and April 1984, the SOUSY-VHF-Radar located in West Germany operated for periods of 16 days and 5 days, respectively, with the goal of obtaining data during one or more frontal passages. In both cases, mesoscale wave structure was observed when weak pressure and temperature gradients dominated at the surface and aloft. The waves appeared as downward-sloping bands of enhanced reflectivities in the altitude range from 0.45 km, the lowest radar range gate, and up to the tropopause. Three to five oscillations were evident. In November 1981, the wave period in the earth-fixed reference frame was approximately 9 hr, while in April 1984, it was closer to 5 hr. The vertical velocities measured with the radar wind profiler showed 30 to 40 cm/s oscillations with the same vertical and temporal structure as the reflectivity bands, although 90° out of phase. The satellite photographs for both periods showed banded cloud structure above the radar.

April 1984

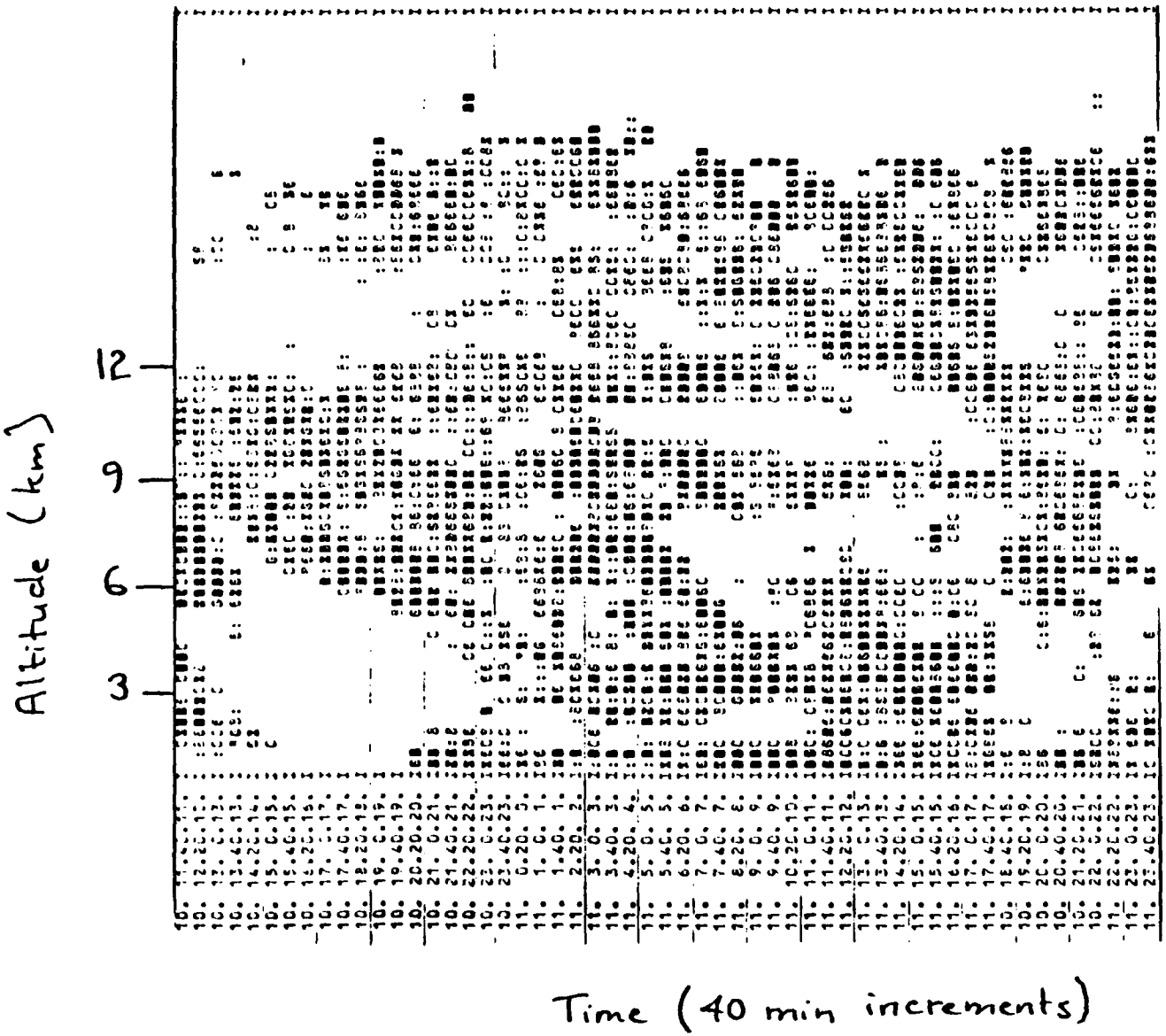

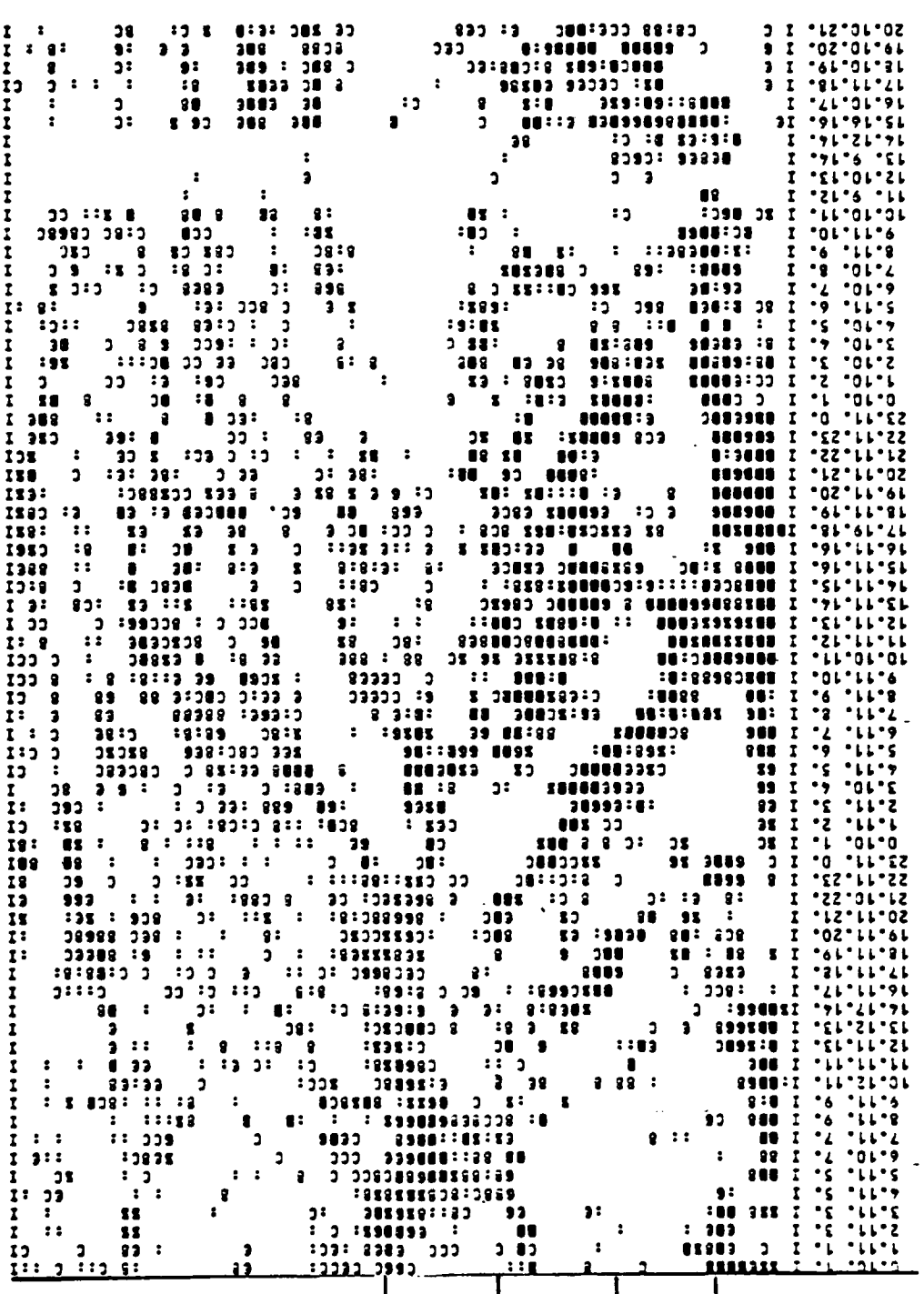
November 1981
Altitude (km)
12
9
6
3
Time (hrs)

END

FILMED

11-85

DTIC